UNIHI-SEAGRANT-CR-77-01

HIG-76-14

FERROMANGANESE DEPOSITS OF THE HAWAIIAN ARCHIPELAGO

By

D. J. FRANK, M. A. MEYLAN, J. D. CRAIG

Department of Oceanography
University of Hawaii
Honolulu, Hawaii 96822

and

G. P. GLASBY

New Zealand Oceanographic Institute
Wellington, New Zealand

DECEMBER 1976

Prepared for
MARINE AFFAIRS COORDINATOR,
STATE OF HAWAII
under Task Orders 21, 28, 35, 43, 44, 45, and 103
and
NOAA OFFICE OF SEA GRANT,
DEPARTMENT OF COMMERCE
under Grants 04-5-158-17 and 04-6-158-44026

HAWAII INSTITUTE OF GEOPHYSICS
UNIVERSITY OF HAWAII

UNIHI-SEAGRANT-CR-77-01 HIG-76- 14

FERROMANGANESE DEPOSITS OF THE HAWAIIAN ARCHIPELAGO

By

D. J. Frank, M. A. Meylan, and J. D. Craig

Department of Oceanography
University of Hawaii
Honolulu, Hawaii 96822

and

G. P. Glasby

New Zealand Oceanographic Institute
Wellington, New Zealand

December 1976

This work is the result of research sponsored by the Marine Affairs Coordinator, State of Hawaii, under Task Orders 21, 28, 35, 43, 44, 45, and 103, and by NOAA Office of Sea Grant, Department of Commerce, under Grant Numbers 04-5-158-17 and 04-6-158-44026. The U.S. Government is authorized to produce and distribute reprints for government purposes notwithstanding any copyright notations that may appear hereon.

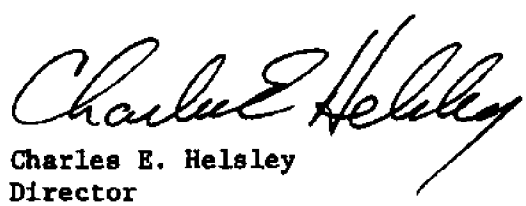

Charles E. Helsley
Director
Hawaii Institute of Geophysics

ABSTRACT

Preliminary surveys by dredging and bottom photography of the submarine slopes and terraces of the Hawaiian Archipelago between the Midway Islands and the island of Hawaii have been made to determine the extent and metal composition of ferromanganese deposits of possible economic importance. The Fe-Mn oxide deposits studied occur mostly at depths of 750-2000 m in the form of stains, encrustations of differing thicknesses (up to about 2 cm), and only rarely as nodules. A variety of solid substrates, including carbonates, have accumulated Fe-Mn oxides, but the thicker deposits are found mostly on altered volcanoclastics and basalt.

The composition of the Mn crusts throughout the archipelago is relatively uniform, and does not seem to vary significantly with crustal thickness, and hence with presumed age. As determined by atomic absorption analysis, the average composition for crusts (1-13 mm thick) from eight stations is: Mn 23.2%, Fe 17.3%, Co 0.86%, Ni 0.40%, Cu 0.04%, and Ti 1.07%. As in deep-sea Fe-Mn nodules, Ni and Cu contents generally increase with higher Mn/Fe ratios. There is a subtle trend of increased Mn, Ni, Cu and Co contents and decreased Fe content along the archipelago toward the northwest. Titanium is, in all cases, less concentrated in the Fe-Mn crusts than in the associated substrates.

Based on X-ray diffraction analysis, the dominant Fe and Mn phases present in the accumulations appear to be amorphous or cryptocrystalline oxyhydroxides. The most common crystalline manganese phase is δ-MnO_2, while todorokite is rarely identifiable. No crystalline authigenic iron phase occurs in recognizable quantities. Plagioclase and pyroxene of probable volcanic origin are commonly admixed with the oxyhydroxides of the Mn crusts, and the alteration products phillipsite and montmorillonite are often noted as well.

The principal metal of economic interest in Hawaiian waters is cobalt, which is present in concentrations four times higher on average than in deep-sea deposits and the cut-off grade for recoverable continental reserves. Nickel and manganese are of potential secondary interest.

TABLE OF CONTENTS

LIST OF TABLES

LIST OF FIGURES

ACKNOWLEDGMENTS

We thank J. E. Andrews, principal investigator for this project. Also our thanks go to M. Morgenstein, who did much of the initial work on this project during its first three years. We appreciate the help of L. Olson, who has provided a great deal of help in sampling and technical operations, both in the laboratory and at sea. Our thanks also go to Ms. L. Fortin who performed all the X-ray diffraction analyses and in general assisted whenever needed.

This project was funded jointly by the Marine Affairs Coordinator, State of Hawaii, and the Sea Grant Program of the University of Hawaii through the Office of Sea Grant, National Oceanic and Atmospheric Administration.

INTRODUCTION

The deposition of ferromanganese oxides in the oceans as nodules and crusts has been under close scrutiny during the past few years and several environments of deposition have been studied (e.g. oceanic seamounts, plateaus, active mid-ocean ridges, inactive ridges, continental borderlands, marginal topographic elevations, and the deep-ocean floor between 2,000 and 6,000 m) (Cronan, in press). These include a number of shallow marine environments such as Loch Fyne, Scotland, Jervis Inlet, British Columbia, the Baltic Sea, the Blake Plateau, the Manihiki Plateau, and the Aghulas Bank (e.g. Manheim, 1965, 1972; Ku and Glasby, 1972; Glasby and Summerhayes, 1975; Summerhayes and Willis, 1975). Archipelagic nodules, however, have been little studied. The Hawaiian Archipelago therefore offers an additional and perhaps unique type of shallow-water marine environment for investigation (see also Morgenstein and Andrews, 1971; Andrews, 1972; Fein and Morgenstein, 1972, 1973, 1974; Morgenstein, 1972a,b, 1973, 1974; Andrews *et al.*, 1973; Landmesser and Morgenstein, 1973; Dugolinsky, 1976).

Ferromanganese deposits in the Hawaiian Archipelago were first described by Moore (1966) in association with volcanic lava flows near the island of Hawaii. Subsequent surveys aboard the R/V Teritu, R/V Moana Wave, and R/V Kana Keoki by the Hawaii Institute of Geophysics for lithified volcanoclastic sediments, and Fe-Mn nodules and crusts, recovered deposits off the coasts of Kauai and Oahu as well as in channels from Kauai to Midway.

The current ferromanganese program at the University of Hawaii, which is studying the shallow deposits of the Hawaiian Archipelago, has been a four-year investigation. This program has been funded by the Marine Affairs Coordinator, State of Hawaii, and the Sea Grant Program of the University of Hawaii through the Office of Sea Grant, National Oceanic and Atmospheric Administration. This program has had two major objectives:

1) To define the extent and resource potential of ferromanganese deposits in the Hawaiian Archipelago and their relationship to age of the island ridges.

2) To investigate the origin of ferromanganese deposits in the "shallow" setting of the Hawaiian Archipelago in order to understand the environmental factors critical to ferromanganese oxide accretion and the enrichment of transition metals in the deposits.

This report is an attempt to summarize the progress and to present the data accumulated to date. In addition, preliminary conclusions have been made concerning ferromanganese deposits in the Hawaiian Archipelago and the economic potential of these deposits. Due to numerous problems

associated with the program during the first three years, only that material which could be reanalyzed or otherwise verified as to quality is included from this period. The remainder constitutes new data. In all cases the data presented represent work performed since January 1976.

GEOLOGY OF THE HAWAIIAN RIDGE

Regional Origin and Structure

The Hawaiian Ridge and its N.N.W. extension, the Emperor Seamount Chain, are genetically related basaltic shield volcanoes that have erupted in Tertiary and Quaternary time across Cretaceous seafloor structural patterns (Jackson *et al.*, 1972). While the eruptive sequence has generally progressed from northwest to southeast, the loci of individual eruptions appear to be non-linear in the southern and best-studied portion of the chain, and occur along sub-parallel (*en echelon*) trends of extensional fault zones in the oceanic crust (Stearns, 1966). Simultaneous eruptions in a 300-km-diameter area suggest a localized upwelling of volcanic material from the mantle, or "hot spot", which has remained approximately fixed beneath a northwestward-drifting Pacific Plate. Individual source areas for magma are estimated to be much smaller (20-km diameter) (Jackson and Wright, 1970). Presently this large "hot spot" is located slightly north of the island of Hawaii. The major bend separating the Emperor Seamounts and Hawaiian Archipelago has been correlated to a vector change in plate rotation about 25 m.y. ago, coinciding with increased tectonic activity along boundaries of the Pacific Plate in the early Miocene (Menard and Atwater, 1968). Seismic refraction studies indicate that the oceanic crust (normally 5-6 km thick) increases in thickness to 10-20 km beneath the Hawaiian Ridge (Furumoto *et al.*, 1965), probably as a result of the transfer of material from the mantle to oceanic crust during volcanic growth. Eruptive sequences of magma types follow a pattern of (1) abundant tholeiitic basalts, (2) minor amounts of alkalic basalt, and (3) rare nephelinite basalts produced in the post-erosional period (Macdonald and Katsura, 1964).

Physiography of the Hawaiian Archipelago

The Hawaiian Archipelago consists of a broad, linear chain of topographic highs on the Hawaiian Ridge. These topographic highs mark the central vent areas of volcanoes and are: (1) submerged and capped by coral in the northwest, (2) deeply eroded in the central portion, and (3) islands in the southeast. Surrounding the major ridge structure is a symmetrical "moat" as much as 0.7 km deeper than the adjacent abyssal Pacific seafloor (Hamilton, 1957), which becomes a sediment trap for materials eroded from the ridge. Geophysical investigations have inferred a subsidence of 2-3 km caused by partial isostatic compensation

of the oceanic crust to the load of this massive pile of volcanic material (Strange et al., 1965). Radiometric dating (K-Ar) has yielded ages of the Hawaiian Islands decreasing from Midway (17.9 ± 0.6 m.y.), Kauai (5.6-3.8 m.y.), Oahu (3.6-2.5 m.y.), Maui (1.3-0.84 m.y.) to Hawaii (1 m.y. to present) (Jackson et al., 1972; Dalrymple et al., 1973, 1974; Clague et al., 1975; Moberly and Larson, 1975; Jackson, 1976) and indicated the very rapid tholeiitic shield-building stage of development. The evolution of the archipelago has generally progressed from (1) a rapid tholeiitic shield-building stage, to (2) an emergent erosional and late volcanic stage, and finally to (3) a subsiding marine erosional and reef-building stage. These evolutionary stages are visible in the landforms of Midway Island (stage 3, atoll), Oahu (stage 2), and Hawaii (stage 1), although transitions between these stages are obviously quite broad.

The ocean floor throughout the archipelago descends in seven sloping terraces which are thought to be glacio-eustatic at depths above 140 m and the result of structural subsidence below 140 m (Stearns, 1974). Intervening slopes are quite steep and rugged (averaging 10^{o}), typical of volcanic terrains, and often consist of major slopes as high as 20^{o} and minor vertical escarpments. Shorelines are recognized either by horizontal notches in rock or narrow deposits of beachrock created during a stillstand of the sea. Submarine shelves are apparently drowned coral reefs overlying wave-truncated basalt platforms (Stearns, 1974). Mathewson (1969) reports six ancient submerged shorelines around the Archipelago: Koko at 5 m, Waipio at 20 m, Penguin Bank at 55 m, Mamala-Kahipa at 90 m, Lualualei from 370-560 m, and Waho at 1100 m.

The first shallow terrace off Kauai, studied by sparker profiling, ranges from less than 90 to approximately 200 m and presumably represents the Mamala-Kahipa stand (Morgenstein, 1974). This terrace contains clastics derived from the island, bioherms, and bioclastic materials. Submarine channels follow the slope between the bioherms, which are primarily composed of ancient reefal detritus. It is assumed that most of these channels are presently active, although some appear to be scars of older drainage networks as indicated by their abrupt appearances in the more shallow terrace areas and their termination on the 12-KHz records on the same terrace. This drainage pattern is evident in the continuation of subaerial distributary patterns and in the appearance of shallower water surge channels and submarine canyons. Most of the streams feeding the bays begin at the Mt. Waialeale drainage divide (Inman et al., 1963).

The second break in slope often occurs at a water depth of approximately 600 m (Lualualei stand) and generally represents the upper limit of a submarine terrace ranging from 600 to 1000 m (Morgenstein, 1974). In most areas it is relatively flat; however, there are zones of rolling hills from 30 to 70 m high. These hills are composed of sediments in bedded sequences, as shown in the sparker profiles. Moreover, some of the channels can be traced back to the present Kauai drainage network while others appear to be discontinuous remnants of previous sedimentary transport patterns.

The Waho Shelf is roughly defined by Morgenstein (1974) (Fig. 2) as a broad platform of 1000- to 2000-m depth, although the deeper limit of the Waho Shelf may be more accurately set at 1600 m. This pseudo-terrace or platform is composed of rolling hills, valleys, fan-shaped lobes of indurated sediments, and submarine channels. The most prominent feature on the Waho Shelf is a volcanic hill located in the south-central portion of the shelf which rises to an approximate water depth of 600 m. The remaining portion of the shelf is relatively flat with relief of between 20 to 100 m. The final and largest break in slope occurs between 1600 and 2000 m, below which an extremely rough slope extends to the channel floor. In general, these same generalizations can be made of most terraces in the Hawaiian Archipelago.

Sediments and Stratigraphy

Sediments in the Hawaiian Archipelago are characteristically composed of volcanoclastics, carbonate bioclastics and coralline limestones, pelagic lutites, and ferromanganese crusts (see also Belshé, 1968). Volumetrically, the bulk of the sediments are volcanoclastics derived from the subaerial deposits on present and past islands in the chain. The 1100-m-deep Waho terrace, generally recognizable throughout the archipelago, contains the most extensive ferromanganese concentrations, though ferromanganese crusts are usually found between 750-2000 m as surficial crusts and buried crustal horizons. Manganese-encrusted sediment samples recovered from the Waho Shelf have been found with partially hydrated basalts as well as volcanoclastic graded beds. Shallower than 750 m, ferromanganese staining is widespread, but does not typically occur in appreciable thicknesses.

Siliceous sponges and samples of gold, pink, black, and bamboo coral have also been recovered in tangle nets during dredging operations. While sponges have been found in almost all dredging stations, the coral is more localized in its distribution. Approximately sixty percent of the sponges recovered have been manganese-stained and contained little fresh organic matter. The remaining sponges were neither manganese- nor iron-stained. Upon recovery, these sponges were found to contain undecomposed tissue.

The deposits on marine terraces and platforms off the island of Kauai can be divided into eight major facies (Fig. 1) based on: (1) observations of impregnated thin sections and smear slides under the petrographic microscope; and (2) observations of undisturbed core and dredge sediments under the binocular microscope (Morgenstein, 1974). These facies are representative of sediments on submarine terraces and shelves throughout the archipelago.

The "high wave energy facies" is composed of volcanic sands and cobbles, with less than 25 percent carbonate clastics. These sediments are confined to the coastal zone where there are minimal reef protection of the shoreline and abundant lava formations at the beach. In portions

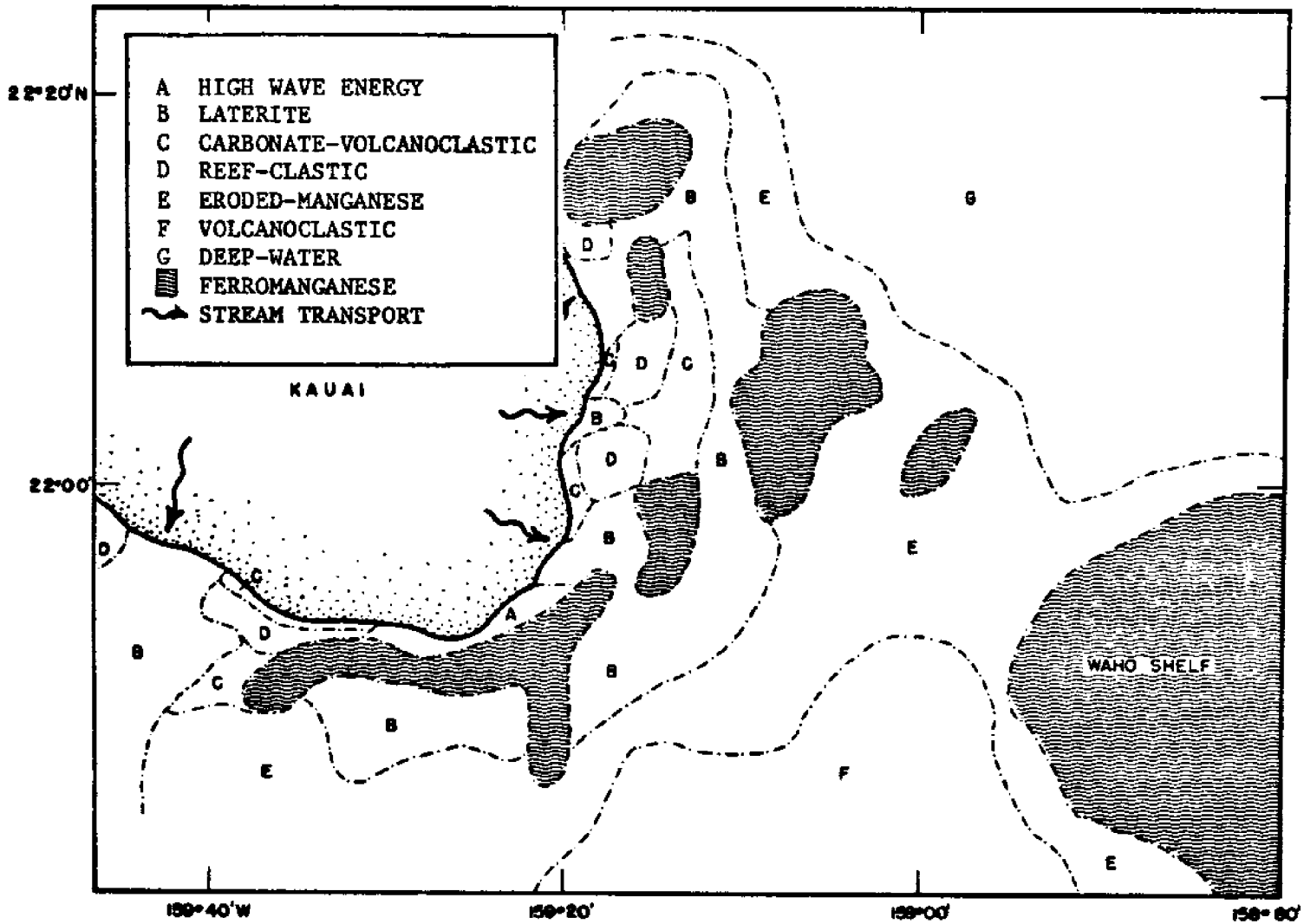

Figure 1. Kauai Channel sediment types (after Morgenstein, 1974).

of the coastal zone, algal balls are observed as massive cobble-sized concretions and are associated with fragments of corals, echnoid spines, gastropods, and benthic foraminifera.

The "laterite facies" is widespread and consists of volcanic sands, silts, and muds originally derived as a result of island stream erosion. This sediment type represents a multi-environment degradation which begins with chemical and physical weathering on Kauai (Walker, 1964), and then undergoes halmyrolysis in the channel. These sediments are deposited in the channel as titaniferous and ferruginous laterites, saprolite rock fragments and bauxitic sapropels, and saprolites.

The "carbonate-volcanoclastic facies" sediments are the result of intermixing of sediment laterite facies and reef-derived carbonates. Carbonate clastics derived from bioherm degradation are mixed with island-derived sediment. Size sorting along the shoreline winnows out the finer volcanic clastics and bioclastics, leaving behind sand-sized debris.

The "eroded manganese facies" consist of manganese crustal rubble, graded and reverse graded sands and silts interbedded with mud laminations, and volcanic sands. The coarser material is of slumped origin and is later reworked and deposited by normal bottom currents. The eroded manganese facies sediments are normally confined to the deeper portions of the channels below the island terraces. The manganese rubble consists of highly abraided, fragmented and fractured remnants of the more shallow crustal zones on the marine terraces.

The "volcanoclastic facies" sediments consist primarily of fine-grained, island-derived detritus with small amounts of pelagic sediments. Most of the sediment can be classified as silty muds with generally less than 10 percent sand-sized debris. The island-derived sediments are mostly palagonite shards, smectites, calcic-feldspars, and reef-derived bioclastics.

The "deep water facies" sediments are similar to the red clays of the Pacific. Pelagic and benthonic bioclastics, illite, iron oxides, and less than 5 percent authigenic mineral components comprise the average sedimentary composition.

The "ferromanganese facies" represent zones of authigenic mineralization, and are primarily manganese crusts interbedded with lithified authigenic sandstones, siltstones, and mudstones. There are occasional manganese nodules with generally large, altered rock fragment centers, and some manganese- and iron-encrusted carbonate sands and silts. The thickness of the ferromanganese crusts has been determined by measuring the average thickness perpendicular to the bedding plane. This thickness varies considerably on the substrates of all of the terraces and there does not seem to be any distinct pattern of crustal thickness. In general, manganese crustal thickness varies considerably over short distances on the Waho Shelf (Morgenstein, 1974). Consequently,

the most frequently occurring thickness observed has been calculated for each dredge haul (Fig. 2). There are two areas located in the northern section of the Shelf which have crustal thicknesses considerably larger than those of the rest of the terrace. These two areas also show anomalously coarse grain size distribution. Crusts in the northwestern portion of the archipelago (leeward islands*) are frequently thicker, having crusts of 1.0-2.5 cm on the average as opposed to an average of 2-5 mm in the Kauai Channel. Volcanic rocks from the island of Hawaii have, at best, thin coatings of manganese oxides. (Moore, 1965, 1966; Moore and Fiske, 1969). This trend is shown in Figure 3, and values are listed in Appendix 1 along with detailed descriptions of the crustal material.

High-frequency sparker profiles were obtained aboard the University of Hawaii's research vessel R/V Kana Keoki during the "Midway 72-07-02" cruise. A continuous seismic reflection profile reveals a relatively thin sedimentary cover above a basaltic basement complex (Fig. 4), although these profiles show considerably thicker sedimentary sections on submarine platforms than on slopes. Sediment thicknesses on these platforms are difficult to determine because of the variable degree of lithification of sediment with depth, occurrence of surficial crusts, and uncertain acoustic velocities. Estimates range from a few tens to hundreds of meters in these terrace sediments. Terrace basement has been identified as either basalt or reefal carbonates by outcrop sampling and seismic reflection studies (Kroenke, 1965).

Stratigraphic distribution of sediments on Kauai Channel terraces is based on samples from three cruises aboard the R/V Teritu where rock cores specially designed to penetrate manganese crusts and indurated sediments were used. The total thickness of the sediment cover above basement cannot be determined from the cores obtained. Moderately successful stratigraphic correlations by lithology and sedimentary structures were attempted from trigger to piston core at each station; however, stratigraphic correlations were not possible between stations due to the inhomogeneity of the sediments and the great distance between stations. Figure 5 exemplifies typical core recovery thickness and stratigraphic positions of various lithologies.

Stratigraphically, the sediments on the terraces consist of interbedded and interlaminated slump units separated by ancient manganese crustal horizons. The slumped sediments seem to conform to the Bouma sequence of turbidites (Bouma, 1963), although their origin has not been documented as such. A reconstruction of the sedimentary events leading to the present stratigraphy is: (1) volcanoclastic slump sedimentation accompanied by bottom current transport and size sorting, (2) bioturbation, (3) sedimentary lithification by ferruginous cementation, (4) ferromanganese crustal accretion, and (5) discontinuous volcanoclastic or slow pelagic sedimentation. The cycle is then repeated.

*The leeward islands are those islands northwest of Kauai.

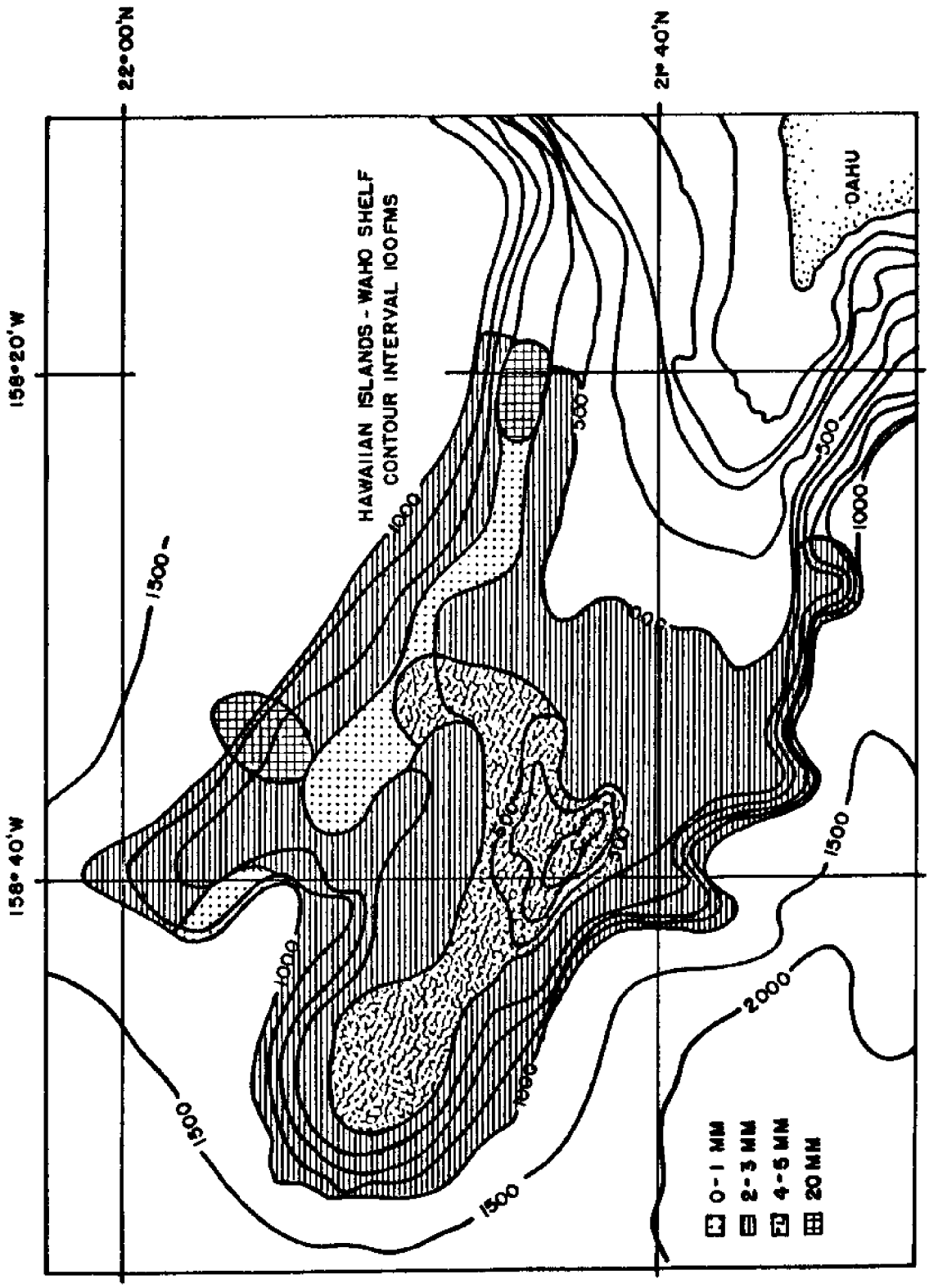

Figure 2. Most frequently occurring thicknesses of manganese crusts on the Waho Shelf (after Morgenstein, 1974).

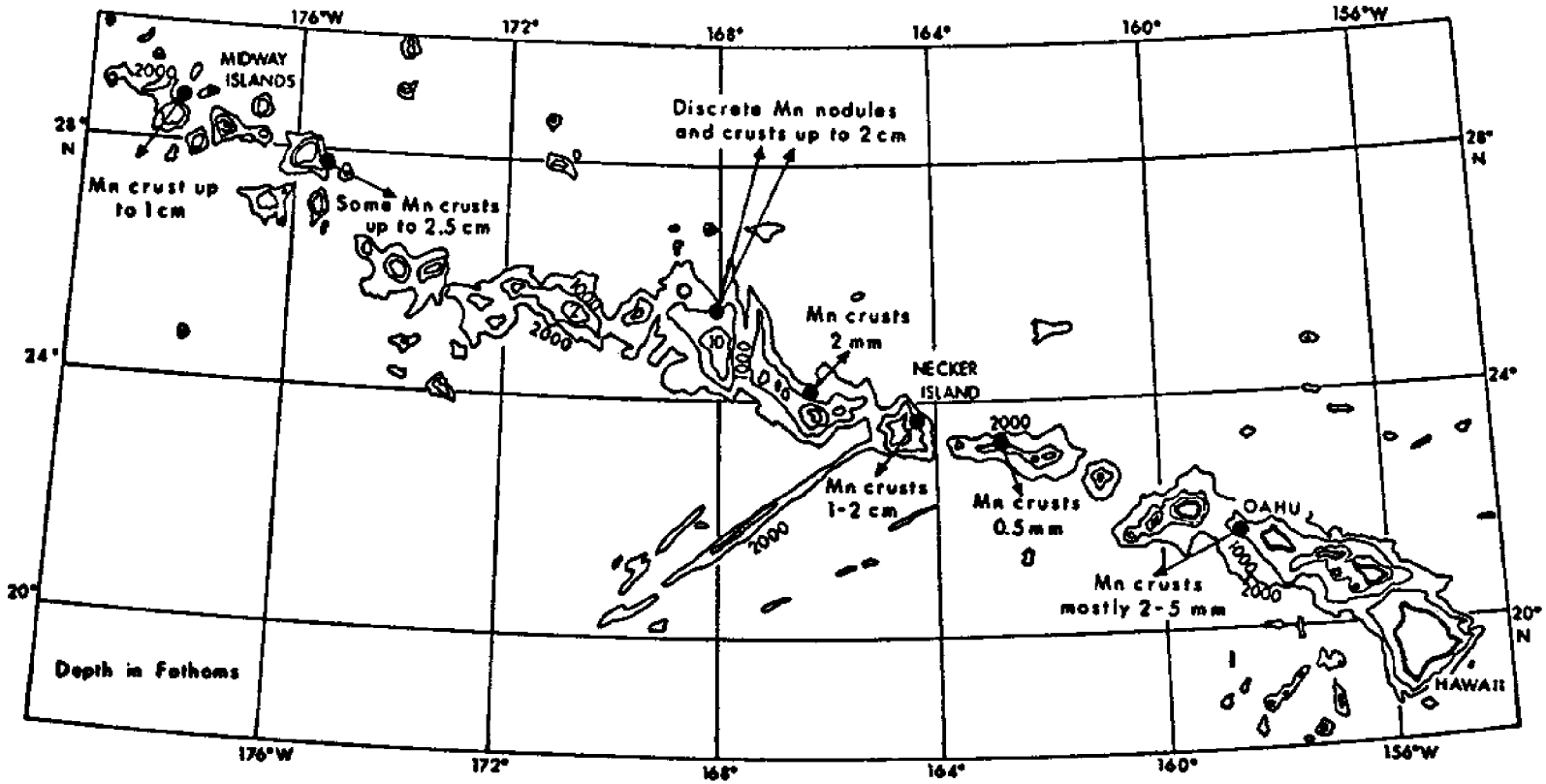

Figure 3. Distribution and thickness of manganese crusts and nodules at individual dredge hauls in the Hawaiian Archipelago.

Figure 4. Seismic profile and line tracing of the Waho Shelf (after Morgenstein, 1974).

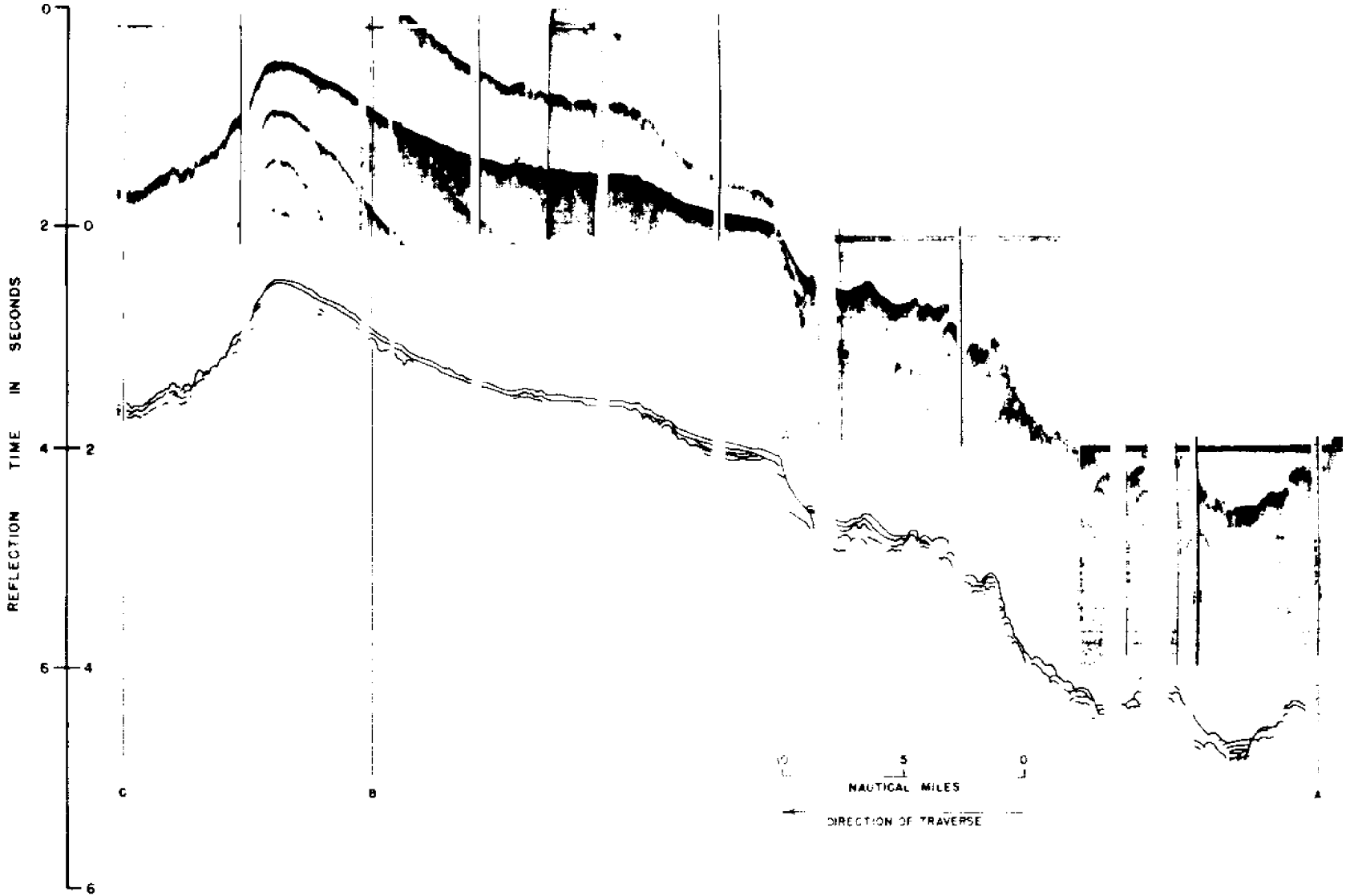
REFLECTION TIME IN SECONDS
0
2
0
4
2
6
4
6
C
B
A
10
5
0
NAUTICAL MILES
DIRECTION OF TRAVERSE

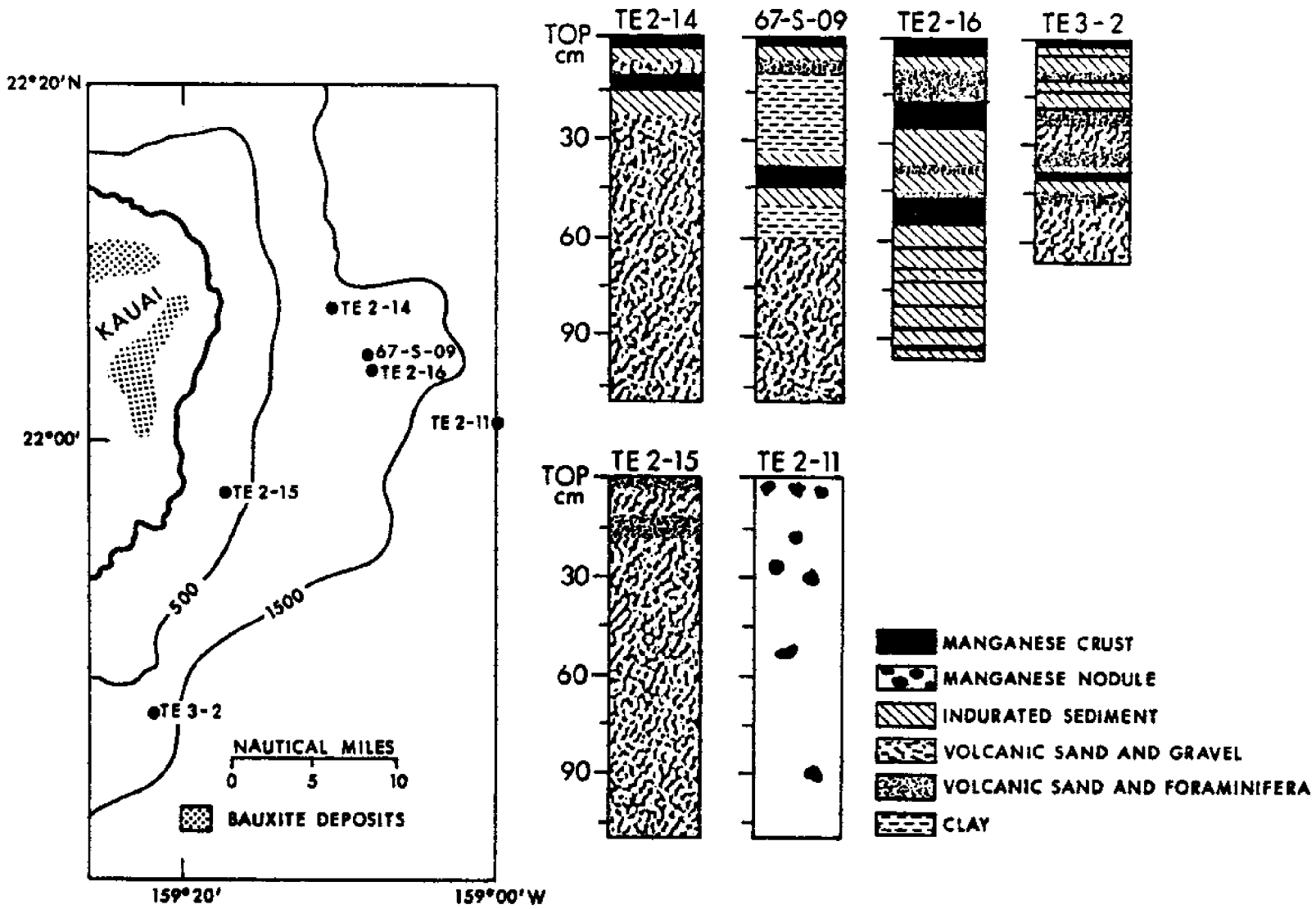

Figure 5. Kauai Channel core stratigraphy (after Morgenstein, 1974).

SAMPLING PROCEDURES

Methods

The earliest surveys carried out in the Kauai Channel (R/V Teritu) incorporated both coring and dredging operations. Rock cores with weight stands carrying 450-730 kgm were allowed to free fall approximately 5 m in order to obtain samples of unconsolidated and semi-indurated sediment. The common occurrence of dense ferromanganese crusts and basaltic outcrops greatly inhibited coring in many areas. The presence of abundant smears and scrapings of manganese on both the weight stand and barrels of cores were indications of ferromanganese crusts in many areas of the terraces, as were deformed cutting heads and core catchers caused by contact with a solid pavement.

Dredges have proved much more useful in sampling these shallow-water ferromanganese deposits. Initial dredging operations employed a single chain-bag or pipe dredge with moderate success. A combined chain-bag and pipe dredge was first used on the Waho Shelf during the summer of 1972, resulting in recovery of samples at 90% of the stations attempted. The chain-bag dredge is attached in front of the system, with a weak link and swivel installed between it and the tow cable from the ship. The pipe dredge is located 1 to 2 m behind, and collects samples broken off the outcrop by the leading dredge. On occasion, large ferromanganese-encrusted boulders were recovered in the chain-bag dredge. Nylon "tangle nets" were frequently positioned beyond the pipe dredge for biologic sampling.

Bottom topography and shallow sub-bottom structure in survey areas have been obtained from continuous reflection profiles using 12-kHz echo sounder and 300-joule sparker systems recorded on Alpine wet-paper recorders. In conjunction with other sampling operations, these reflection profiles have provided useful data relating to the distribution of ferromanganese deposits and the submarine geomorphology in the Hawaiian Archipelago.

The most recent (Mn 75-02) survey utilized bottom photographs obtained using an Edgerton deep-sea camera system along with dredge sampling in the same area. During this survey, the camera frame was "flown" about 3 m above the seafloor and the seafloor photographed at 10-second intervals. At drifting speeds averaging about 0.9 to 1.8 km/hr, these camera traverses produce excellent coverage of one photograph every 5 to 10 m of seafloor. Ship's navigation (obtained by celestial fixes, dead-reckoning, and satellite navigation) during these periods cannot produce the accuracy necessary to map the seafloor directly using bottom photographs; however, as a reconnaissance technique, bottom photographic surveys are far superior to the previously mentioned dredging and core sampling methods. Difficulties in flash synchronization and maintaining the proper focal distance of 3 m resulted in a typical yield of negatives, 20% to 60% of which were useful. Future use

of a bottom camera sled should eliminate these problems in addition to providing oblique-angle photographs that represent the bottom geomorphology more accurately.

Submarine Photography

Recent developments in marine science have stressed the necessity of direct observations of processes affecting the submarine environment. The difficulties of remote sensing in the deep sea have been surmounted by a variety of vehicles, most of which employ some means for recording the bathymetry on photographs on video tape. This method of in situ observation has resulted in many discoveries and, perhaps more importantly, "a feel" for this type of setting.

The bottom photographs included in this report represent an initial attempt at correlating the sampling efficiency of dredging with the actual occurrence of ferromanganese-encrusted substrate in the waters off the Hawaiian Islands. Previous survey work has stressed the necessity for gathering material for chemical analysis without seriously considering the bathymetric distribution of ferromanganese crusts or the micro-relief features found associated with these crusts. This relationship appears to be very important in theories relating to the genesis of the ferromanganese material.

As seen in Figures 6, 7 and 8 from the Mn 75-02 cruise, ferromanganese oxides encrust literally all hard substrate areas, although as previously stated, these crustal thicknesses may vary significantly over short distances on the seafloor. Most rock outcrops appear to be disintegrating into boulder- to pebble-sized fragments, which in turn are dispersed and become substrates for further ferromanganese accretion. Another striking feature of the bathymetry is its ruggedness--on a scale of meters as revealed by these photographs to a larger scale of tens to hundreds of meters as recorded on echo sounding profiles. There is, however, a similarity of sediment/rock outcrop geomorphology between terrace areas of low relief (Fig. 7) to those of rugged slopes (Fig. 6). Sediment distribution in most of the photographs appears to be patchy and sediments often occur as a thin veneer covering harder underlying substrate. Evidence for transport of sediment by bottom currents is occasionally visible in areas of little bathymetric relief (Fig. 7), although the existence of these currents has not been documented to date. The absence of bottom-dwelling fauna in these photographs is surprising considering the proximity to land, water depth, and environmental complexity. The presence of benthonic organisms could be inhibited by the coarse-grained nature, limited distribution, and mobility of the sediment patches, and this in turn could affect other trophic levels.

Similarity in photographs from contrasting bathymetric settings is created, in part, by the technique used in bottom photography. Because of the variable distance of the camera to the seafloor, scales are not

Figure 6. Bottom photographs from Camera Station No. 1, Mn 75-02. ($21^{\circ}54'N$, $158^{\circ}40'W$, 1770 m, Kauai Channel)

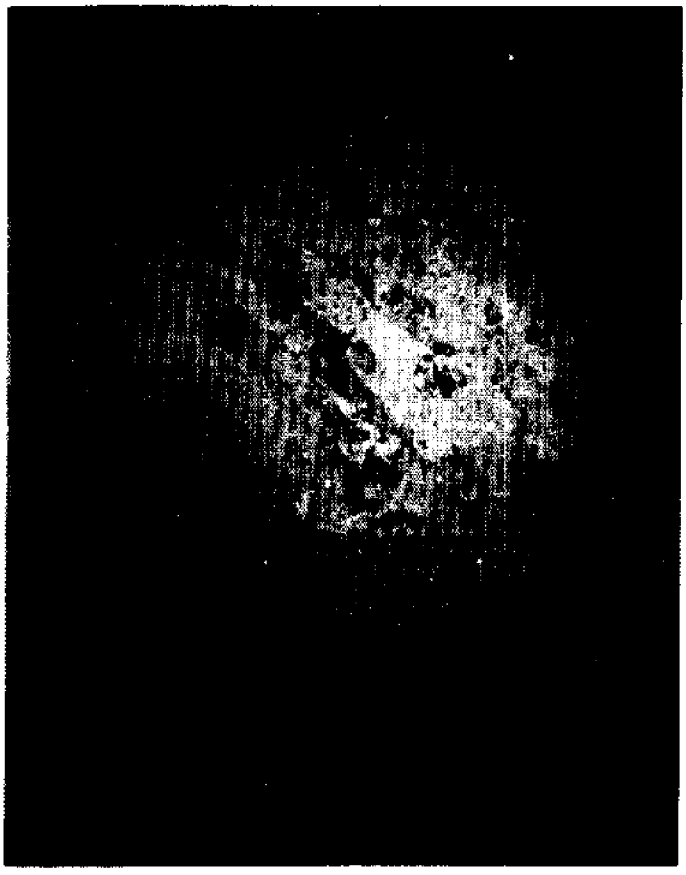

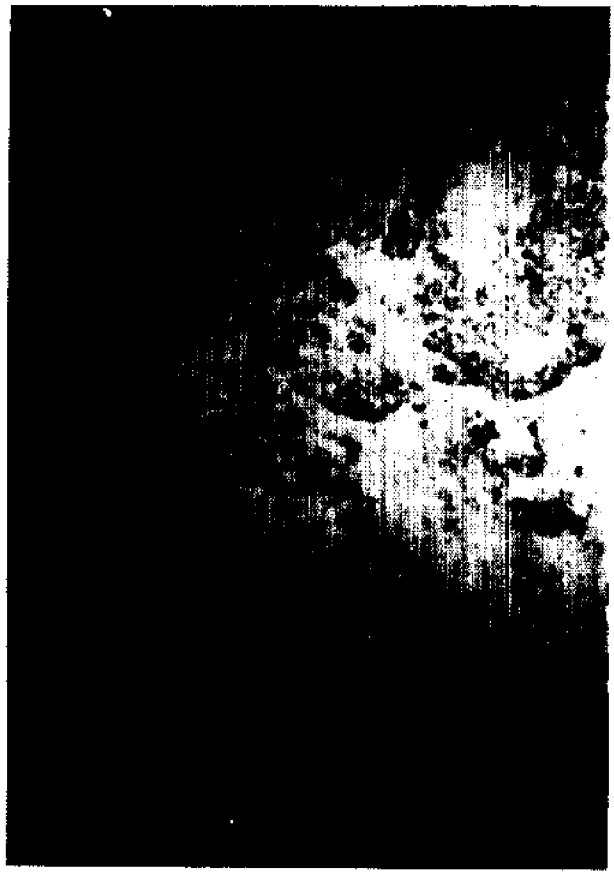

Figure 7. Bottom photographs from Camera Station No. 3, Mn 75-02. ($21^{\circ}42'N$, $158^{\circ}35'W$, 985 m, Kauai Channel)

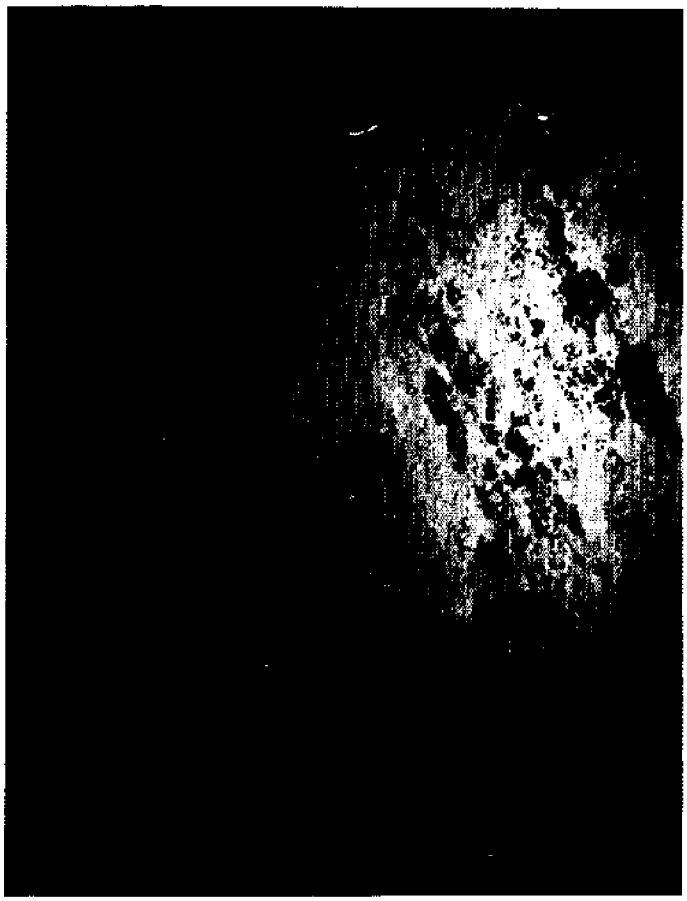

Figure 8. Bottom photographs from Camera Station No. 5, Mn 75-02. ($20^{\circ}06'N$, $156^{\circ}16'N$, 1420 m, off western coast of island of Hawaii)

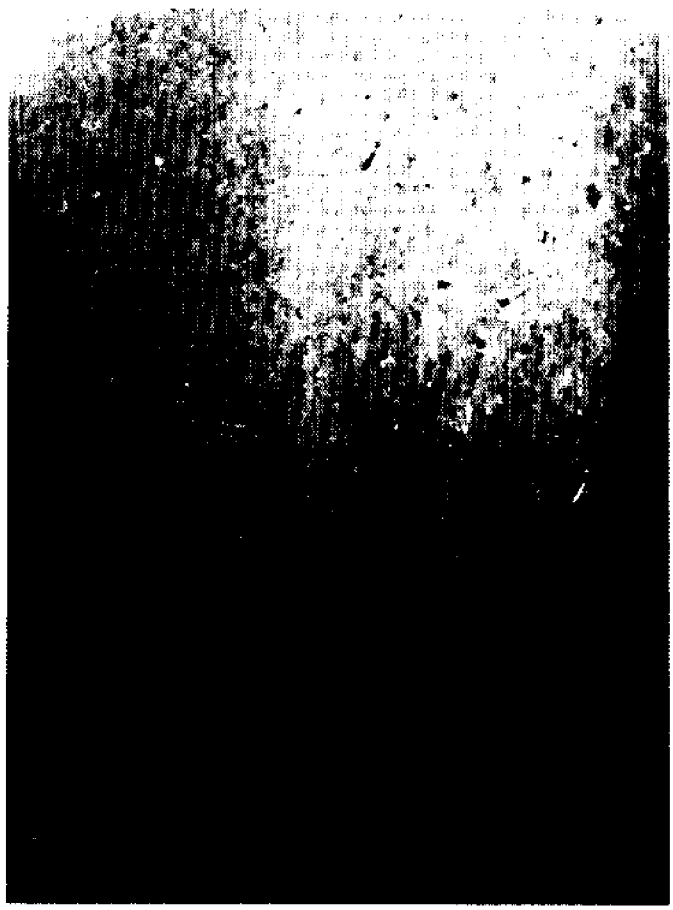

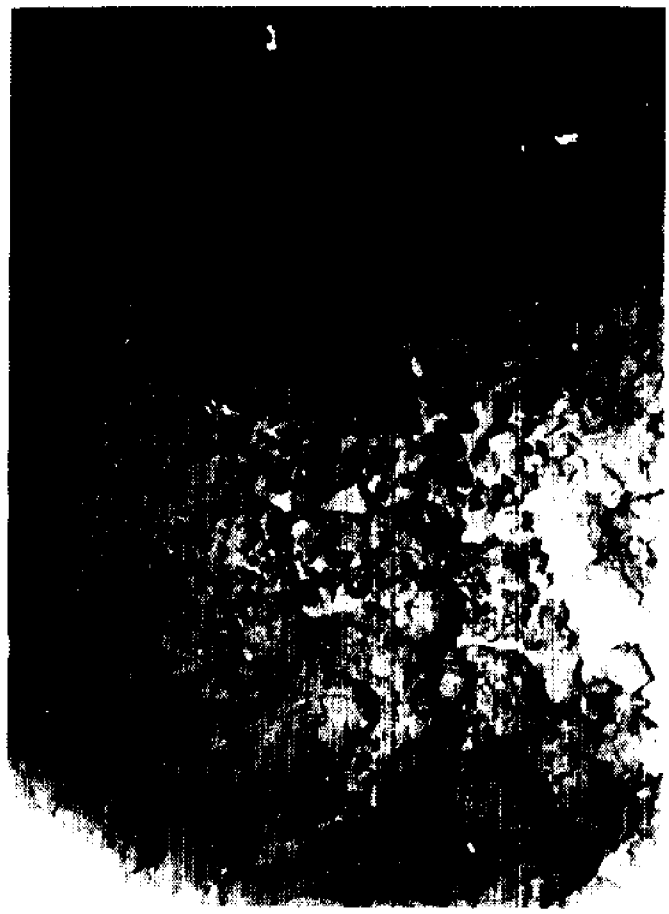

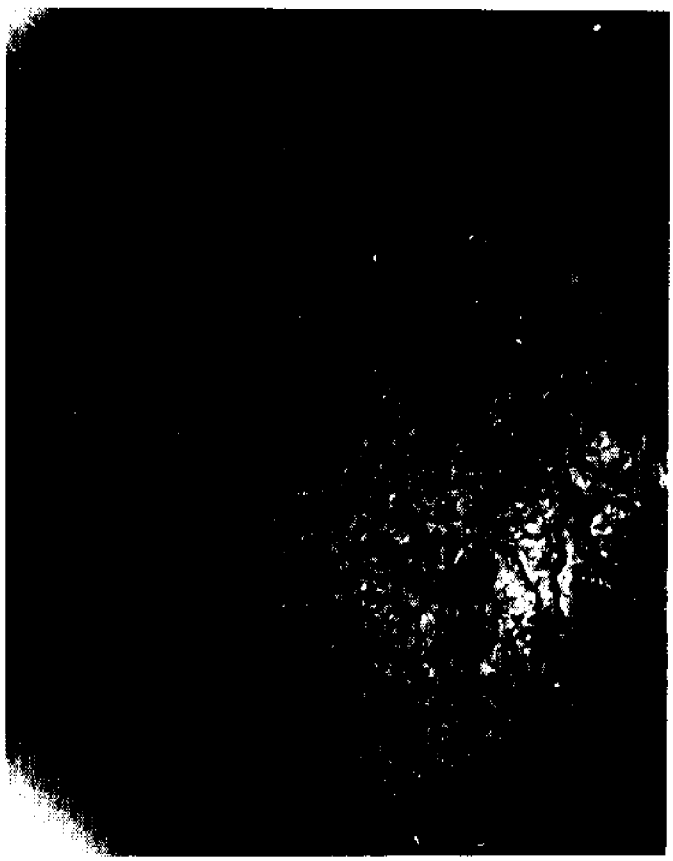

uniform in all photographs, causing a distortion in size and shape of visible objects. In addition, a "vertical aspect" limits the depth of field perspective and creates the illusion of "flatness" even on very rough slopes. An accidental rotation of the camera frame in Figure 7 provides a much more realistic and useful observation of submarine relief. In the future, utilization of a camera sled towed along the seafloor with two camera systems will provide this interesting oblique aspect for distant shots, as well as constant focal length for true scale determinations in close-up shots. An additional advantage of the camera sled over a "flown" camera is that a pinger is unnecessary for its operation. The ship's echo sounding system can be used simultaneously with camera traverses, thus providing a direct bottom profile on which the occurrence of sediment and ferromanganese crusts can be mapped very accurately. This significant improvement will allow the survey method of dredging and bottom photography at the same sites to provide a more accurate evaluation of ferromanganese occurrence and composition in the Hawaiian deposits.

Sample Description

The samples used in this study were selected from KK-72 Midway, Moana Wave and Mn 75-02 dredge collections of the Hawaii Institute of Geophysics. The selection, description, and all analytical measurements of the samples were made between January 1976 and June 1976 with the exception of those from Moana Wave I expedition. The Moana Wave I samples had been previously analyzed; however, due to incomplete sample descriptions and inconsistent data treatment for material analyzed prior to January 1976, these samples had to be reanalyzed. In addition, data from other samples (approximately 25 ferromanganese crusts and associated substrates) from this period have not been included for the above reasons plus the fact that the original samples could not be located for verification of previously reported data. Descriptions for all samples used in this study are given in Appendix 1. In addition, figures 9 and 10 show charcoal drawings of two representative ferromanganese accumulations of the Hawaiian Archipelago.

MINERALOGY

The mineralogy of ferromanganese oxide accumulations and their accompanying substrates was determined by X-ray diffraction. Samples were powdered and portions of the powders set aside for chemical analysis. X-ray diffraction was accomplished with a Phillips X-ray generator, goniometer, and pulse height analyzer. The sample powder was packed into an aluminum planchet and subjected to nickel-filtered Cu-Kα radiation (at 50 KV, 20 ma) during 1^{o} 2θ/minute scans from 3^{o}-60^{o} 2θ. Each sample was run three times to check the reproducibility of smaller peaks. The intensity of the diffracted X-ray beam was recorded on a strip chart, and mineral identifications were based on the recorded peak positions and relative intensities. High iron and manganese contents

Figure 9. KK-72 Midway DG 32. Oblique cross-sectional view of tabular manganese nodule. This portion of nodule is 10 x 10 x 4.5 cm. Note well developed (high relief) botryoids on upper side of nodule, with individual botryoids up to 1 cm in diameter. Upper Mn crust is about 1 cm thick. Nucleus is buff-colored tuffaceous siltstone displaying blocky fracturing.

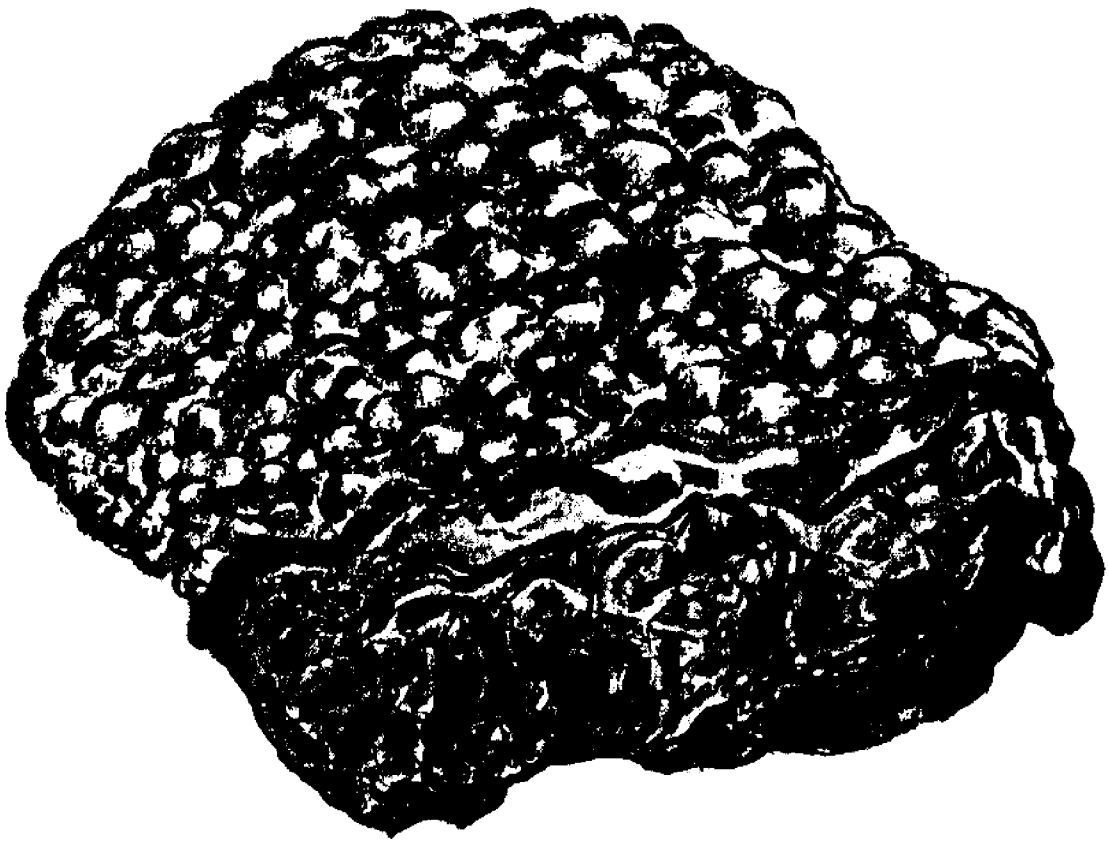

K K 7 2 Midway D G 3 2

Figure 10. KK-72 Midway DG 43. Oblique cross-sectional view of fragment of manganese crustal accumulation. Fragment is 9 x 9 x 4 cm. Note that large botryoids on the upper surface have a more suppressed relief than those of KK-72 Midway DG 32. Mn crust is about 0.5 cm thick. Nucleus is a buff-colored tuffaceous siltstone that is prominently burrowed.

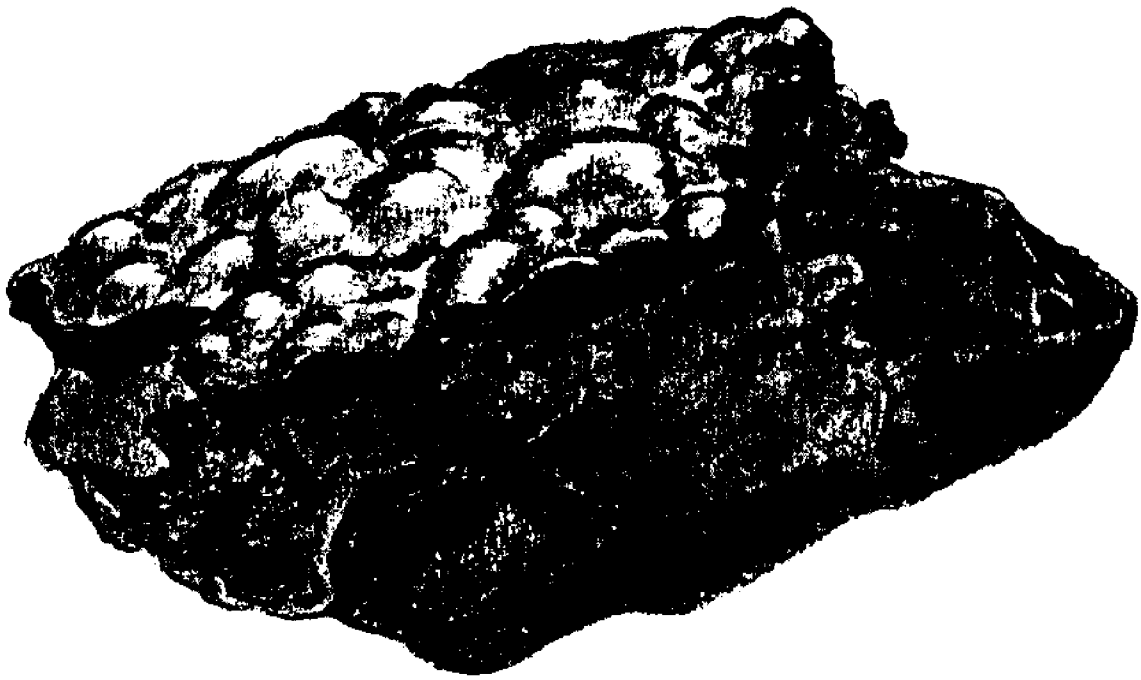

KK 72 Midway DG 43

produced a high fluorescence background. This, combined with the multitude of peaks attributable to the more common minerals, tended to obscure those minerals present in amounts of less than several percent. Table 1 summarizes the minerals identified by X-ray diffraction in Hawaiian marine manganese deposits. Appendix 2 lists the results of all mineralogical analyses.

TABLE 1

MINERALOGY OF HAWAIIAN MARINE MANGANESE DEPOSITS
BASED ON X-RAY DIFFRACTION ANALYSES

FERROMANGANESE CRUST	
Dominant	X-ray amorphous Fe, Mn oxides and hydroxides
Common	δ-MnO_2, substrate minerals
Rare	Todorokite
SUBSTRATE	
Dominant	Plagioclase feldspar, pyroxene
Common	Calcite, phillipsite, montmorillonite, quartz, volcanic glass(?), olivine, illite
Rare	Aragonite, goethite, maghemite and/or magnetite, kaolinite, ilmenite(?), hematite(?)

The bulk of the iron and manganese oxides and hydroxides present in Hawaiian Archipelago ferromanganese crusts occurs in X-ray amorphous forms, i.e., the iron and manganese are so finely divided or structurally inhomogeneous that they do not produce a coherent diffracted X-ray beam. However, substantial amounts of iron can be present in other mineral phases when substrate material is admixed with the oxide crusts. Pyroxene, an iron-bearing silicate, is an abundant mineral in basaltic substrates, and olivine, another silicate common in oceanic volcanic rocks, probably also contributes iron. Montmorillonite, derived from the submarine weathering of volcanic rocks, may be present in the form of nontronite, which contains iron in its structure. Small amounts of the iron oxides magnetite and/or maghemite appear to be present in the substrate samples DG 33C and DG 43B from the KK-72 Midway cruise, and are probably present, but obscured, in most other substrates. Ilmenite, an iron-titanium oxide, is a common accessory mineral in basalt, but seldom occurs in quantities recognizable by X-ray diffraction analysis.

Goethite, an iron oxyhydroxide, was identified as a major constituent in sample DG 48B, but was not identified in any other sample.

The dominant crystalline manganese oxide is δ-MnO_2, which apparently occurs in all ferromanganese crust accumulations, and is probably epitaxially intergrown with $FeOOH \cdot nH_2O$ (Burns and Burns, 1973). Todorokite, the Mn oxide $[(Na, Ca, K, Ba, Mn^{2+})_2Mn_5O_{12} \cdot 3H_2O]$ that appears to concentrate Ni and Cu in deep-sea nodules, was definitely identified in only two of the Hawaiian Archipelago samples studied (MW1-12 #14A and KK-72 Midway DG 24). The formation of todorokite appears to be enhanced by high Mn/Fe ratios (Meylan and Goodell, 1976), that characterize these two samples, but it is somewhat surprising that todorokite is not present in Mn 75-02 #17, a sample with a high Mn/Fe ratio and relatively high concentrations of Ni and Cu. Possibly the iron content, which is about twice that reported in todorokite-rich deep-sea nodules from the economically-attractive deposits of the northeastern equatorial Pacific, ties up too much of the manganese in δ-MnO_2/$FeOOH \cdot nH_2O$ epitaxial intergrowths to permit identifiable proportions of todorokite to form.

The ferromanganese oxide crusts precipitate primarily on nuclei or substrates of basaltic volcanic rocks, which consist mostly of plagioclase feldspars, pyroxenes and glass(?), the latter undetectable by X-ray diffraction except in large quantities. Often the basaltic substrate will be weathered to some degree, as indicated by the presence of authigenic montmorillonite and phillipsite. Other clay minerals such as illite or kaolinite often make up a significant fraction of the substrate, while basaltic volcanics contribute minor amounts of olivine, magnetite and/or maghemite, ilmenite(?) and hematite(?). Quartz, an ubiquitous mineral in the marine environment, is probably contributed by eolian transport from continental land masses (Dymond et al., 1974). Thin ferromanganese oxide crusts also form on organic substrates such as coral (consisting of the minerals calcite or aragonite) or sponges (X-ray amorphous opal).

Selected X-ray diffraction traces of oxide crusts and substrates are presented in Figures 11 and 12. The uppermost trace of Figure 9 shows evidence of the presence of todorokite, i.e., from right to left, broad peaks at 9.6 Å, 4.85 Å and about 2.4 Å. The lowermost trace of Figure 11 is more typical of Hawaiian marine manganese crusts, i.e., only the very broad peak of δ-MnO_2 at about 2.4 Å (shared with todorokite) is present (although in some samples there are peaks attributable to one or more substrate minerals which have been incorporated into the crust). Figure 12 illustrates substrate diffraction mineralogy. The uppermost trace is somewhat atypical in that other samples do not contain identifiable quantities of calcite and montmorillonite in addition to the typical plagioclase feldspar/pyroxene assemblage. The middle trace was produced by the substrate most enriched in montmorillonite, while the lowest trace is from the only substrate with definite goethite and magnetite/maghemite peaks.

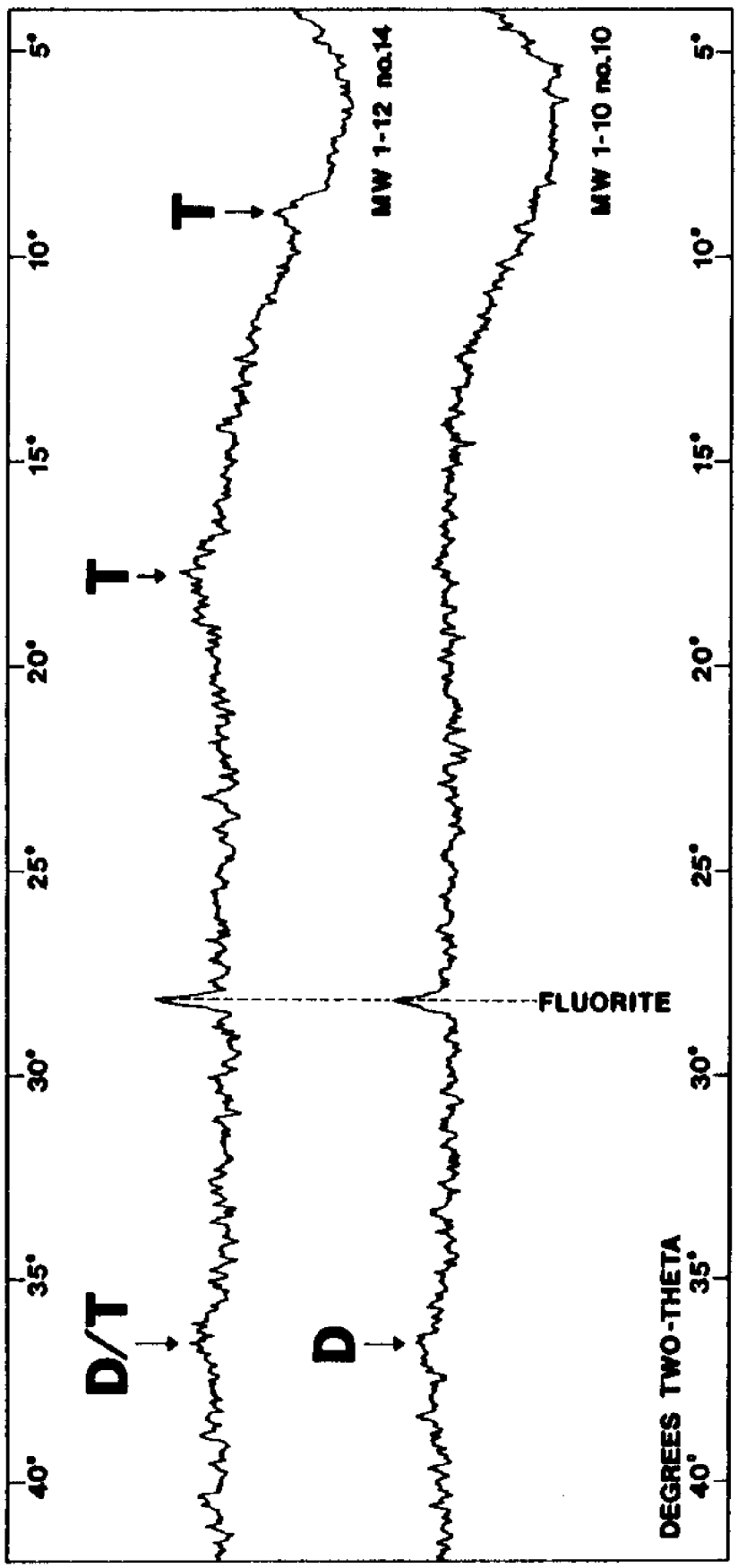

Figure 11. X-ray diffraction traces of Hawaiian marine ferromanganese oxide crusts. T = todorokite. D = δ-MnO_2. Fluorite added as internal standard.

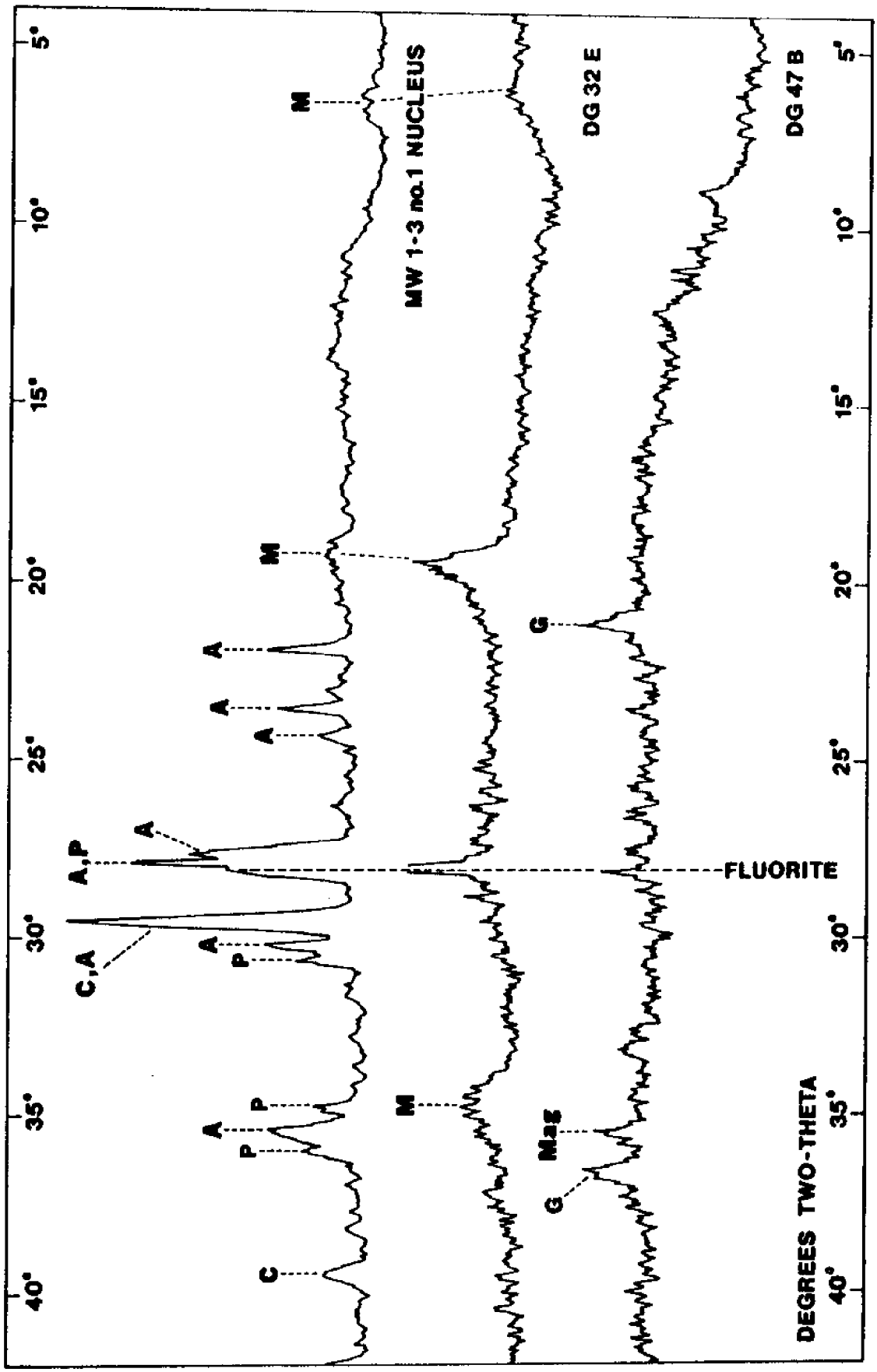

Figure 12. X-ray diffraction traces of substrates onto which ferromanganese oxide crusts accumulated. A = plagioclase feldspar, C = calcite, G = goethite, M = montmorillonite, Mag = magnetite/maghemite, P = pyroxene. Fluorite added as internal standard.

CHEMISTRY

Analytical Procedures

The chemistry of the ferromanganese oxide accumulations and their accompanying substrates was determined by two methods. Atomic absorption spectrophotometry was used for the analysis of Fe, Mn, Al, Co, Cu, and Ni, while Ti was determined by X-ray fluorescence (XRF) using Energy Dispersive Analysis of X-rays (EDAX). The atomic absorption work was carried out by D. J. Frank in the laboratory of Dr. B. J. Presley at the Department of Oceanography, Texas A & M University. The EDAX work was carried out at the University of Hawaii.

Procedures used for the total dissolution of the powdered samples for analysis by atomic absorption were modified from those of Jeffrey (1970). Approximately 0.3 g of the dried sample was weighed into a Teflon beaker. Each sample was then treated with ∿3 ml Aqua Regia (1 ml 16N HNO_3 and 2 ml 6N HCl) and the solution heated on a hotplate for 1-2 hrs. After evaporation to ∿½ ml volume, 5 ml HF (48%) and ½ ml $HClO_4$ were added to the sample. The beakers were then covered with Teflon covers and allowed to reflux for 8 hrs. Next the solution was allowed to evaporate until all HF had been driven off and the $HClO_4$ began to fume (∿ ½ ml). At this point 5 ml distilled H_2O was added and the hot solution was transferred to a 25-ml measuring cylinder and diluted to volume when cool. For samples which were difficult to dissolve (due to high Fe and Mn contents), an additional treatment with Aqua Regia proved effective after evaporation of the HF. Samples were prepared in batches of thirty and a reagent blank was always processed along with the samples. A number of replicate samples were analyzed in each batch and a number of samples were reanalyzed from one batch to another as a check on precision. After appropriate dilutions all samples were analyzed on a Jarrell-Ash model 810 atomic absorption spectrophotometer. The analytical wavelengths used for measurement were those recommended by the manufacturer. Standards were prepared in 1N HNO_3 from Hartman-Leddon standard reference solutions. The effect of background absorbance was found to be negligible for Fe and Mn due to their extreme dilution (∿ 80,000x). However, the background for Al, Co, Cu, and Ni was corrected for by measuring the absorbance at a non-absorbing wavelength in addition to the absorbance at the analytical wavelength of interest.

Samples for the analysis of Ti were prepared by first grinding to a uniform powder (∿ 100 mesh). Next, approximately half of the samples were mixed with an equal amount of boric acid (reagent grade) and pressed into aluminum planchets at ∿690 bar (10,000 psig). The remainder of the samples was pressed into planchets as pure powders. Results showed no difference between these two methods as determined from samples analyzed by both methods. The prepared samples were then subjected to X-rays from a Rhodium source operated at 20 KV and 32 ma. Each sample was irradiated and the fluorescent X-rays corresponding to the Ti Kα line were counted. Each sample was counted three times and the results

averaged. A few replicate samples were analyzed as a check on precision. The standards used were Fe-Mn oxides previously analyzed by atomic absorption and XRF analysis by Meylan (1968). These samples were chosen as standards since their elemental compositions closely matched those of the oxides under study and therefore would present similar matrix and inter-element effects on irradiation. Additional matrix and inter-element interferences were corrected by using curve smoothing and background subtraction programs on the mini-computer built into the EDAX system.

For both atomic absorption and X-ray fluorescence, known samples were analyzed in addition to the Fe-Mn crusts and substrates to provide an estimate of the analytical precision and accuracy. Table 2 compares the results obtained for the Marine Standard Nodule GRLD-126 with those from other laboratories. These data show that the analytical accuracy and precision obtained (number 14 in table) is comparable with that obtained by other investigators using various methods. In addition to this standard, a number of previously analyzed samples were analyzed and the results are presented in Table 3. The data from these tables plus the results of replicate analysis indicate an overall average accuracy and precision of 5-10% of the reported value.

Results and Discussion

In selecting samples for analysis there was always a problem of obtaining a portion of the ferromanganese crusts that was uncontaminated by substrate material. In some cases this proved to be impossible due to the fact that the crust was either too thin to be cleanly separated or the crust and substrate were intergrown to too great a degree. Consequently all averages of elemental abundance in the crustal materials have excluded those samples in which a substantial amount of substrate was present.

The results of the chemical analysis of the ferromanganese crust and their associated substrates are presented in Appendix 3. Elemental averages were made for each area of the Hawaiian Archipelago from which samples were obtained. These averages are shown in Figures 13 and 14. Although the sample coverage is incomplete, a slight trend toward increasing Co, Cu, Ni, and Mn and decreasing Fe and Ti concentrations can be seen toward the leeward islands. However, additional data are needed to substantiate this trend fully.

There are few well-defined inter-element trends observable except for an inverse correlation of Co with Al. In the manganese crusts, Mn shows a good correlation with Co, a poor correlation with Ni, no correlation with Cu, and a poor inverse correlation with Fe. The poorly defined correlations may be due in part to a lack of quality samples over the extremely large area of the Hawaiian Archipelago. Future sampling expeditions, in particular those concentrated in the leeward island chain, should help to clarify this anomaly. The inverse

TABLE 2

CHEMICAL ANALYSIS OF MARINE STANDARD NODULE GRLD—126

Element	Acid-soluble Fraction of Sample								Total Sample					
	1	2	3	4	5	6	7	8	9	10	11	12	13	14
Fe (wt.%)	8.66(0.12)	9.71(0.30)	10.8	9.94	9.5	10.4	9.06	9.55(0.15)	9.77(0.23)	10.6	10.37(0.44)	10.32	10.6(0.5)	9.4
Mn (wt.%)	23.6(1.5)	22.88(0.34)	23.7	23.68	22.9	25.1	23.5	22.65(0.23)	24.7(0.7)	25.2	23.09(0.22)	24.44	25.5(1.0)	24.4
Cu (wt.%)	0.592(0.018)	0.641(0.009)	0.59	0.626	0.65	0.62	0.67	0.609(0.014)	0.630(0.060)	0.669	0.670(0.030)	0.605	1.02(0.25)	0.66
Ni (wt.%)	0.760(0.011)	0.941(0.019)	0.85	0.993	0.92	1.03	0.59	0.929(0.087)	1.00(0.04)	1.05	0.988(0.070)	1.09	1.25(0.25)	1.01
Co (ppm)	1350(29)	1487(30)	1400	1550	9300	1130	1800	1524(43)	1380(50)	1600	1437(26)	2408	NA	1578
Zn (ppm)	1217(28)	1274(15)	1330	NA	1415	NA	1630	1220(16)	3700(400)	NA	1276(22)	NA	1400(500)	NA
Ca (wt.%)	1.38(0.02)	1.36(0.01)	1.3	1.43	1.36	NA	NA	1.28(0.02)	NA	1.58	1.29(0.001)	1.46	1.42(0.11)	NA
Mg (wt.%)	1.33(0.02)	1.41(0.03)	1.3	1.53	1.67	NA	NA	1.53(0.02)	NA	1.80	1.51(0.024)	0.87	0.72	NA
Na (wt.%)	2.81(0.11)	1.71(0.06)	1.9	1.94	1.66	NA	NA	NA	1.84(0.06)	2.15	NA	1.93	NA	NA
K (wt.%)	0.82(0.01)	0.59(0.02)	0.9	0.99	0.76	NA	NA	NA	NA	1.04	NA	0.93	1.55(0.11)	NA
Si (wt.%)	NA	NA	NA	NA	NA	NA	NA	NA	NA	NA	NA	NA	9.78(0.97)	NA
Al (wt.%)	NA	NA	NA	NA	NA	NA	NA	NA	NA	NA	NA	NA	2.50(0.35)	2.5
Ti (wt.%)	NA	NA	NA	NA	NA	NA	NA	NA	NA	NA	NA	NA	0.32(0.08)	NA

Values in parentheses are standard deviations; NA = not analyzed.

1 - Michigan-1973 (Callender/Roberts), 10% HCl-30% H_2O_2 soluble; atomic absorption.
2 - Michigan-1975 (Callender/Shedlock); 10% HCl-30% H_2O_2 soluble; atomic absorption.
3 - Miami (Joensuu); spectrograph.
4 - Kennecott; acid soluble; atomic absorption.
5 - Syracuse (Dean); concentrated HCl soluble; atomic absorption.
6 - Wisconsin-1973 (Morgan); concentrated HCl-$HClO_4$ soluble; atomic absorption.
7 - Washington (Piper); acid soluble; neutron activation/atomic absorption.
8 - Wisconsin-1975 (Bowser); 10% HCl-30% H_2O_2, 25% hydroxylamine-hydrochloride dithionate-citrate; atomic absorption.
9 - Battelle NW (Rancitelli); total sample; neutron activation.
10 - Kennecott; HF, HNO_3, HCl, $HClO_4$ digestion; atomic absorption.
11 - Wisconsin-1975 (Bowser); HF-boric acid digestion; atomic absorption.
12 - Hawaii (Fein); Li-tetraborate fusion, HF-HNO_3 digestion; atomic absorption/X-ray fluorescence.
13 - Hawaii (Dugolinsky); total sample; X-ray fluorescence.
14 - Hawaii (Frank); HF-HNO_3, $HClO_4$ digestion; atomic absorption.

TABLE 3

COMPARISON OF PREVIOUSLY ANALYZED AND REPLICATE SAMPLES

Sample	Method	Number of Analyses	WEIGHT PERCENT Fe	Mn	Al	Co	Cu	Ni	Ti
7M	XRF & A.A. (Meylan, 1968)[a]	1	18.9	19.1	---	0.19	0.19	0.46	0.71[e]
	A.A. (Frank, this work)	1	23.3	22.3	---	0.18	0.21	0.41	---
33M	XRF & A.A. (Meylan, 1968)[a]	1	12.1	22.6	---	0.46	0.36	1.03	1.00[e]
	A.A. (Frank, this work)	1	12.9	23.7	---	0.39	0.43	0.90	---
35M	XRF & A.A. (Meylan, 1968)[a]	1	16.8	21.9	---	1.02	0.06	0.37	1.29[e]
	A.A. (Frank, this work)	1	20.4	24.4	---	0.91	0.11	0.38	---
50M	XRF & A.A. (Meylan, 1968)[a]	1	24.7	14.1	---	0.10	0.21	0.49	0.24[e]
	A.A. (Frank, this work)	1	25.6	15.0	---	0.08	0.24	0.35	---
74-1 FFC002	XRF (Dugolinsky, 1975)[b]	3	7.3 ± .6	29.9 ± 1.9	2.7 ± .6	---	1.27 ± .02	1.55 ± .09	0.46 ± .05
	A.A. (Frank, this work)	3	6.3 ± .6	30.5 ± 1.9	2.7[c]	0.21 ± .01	1.37 ± .09	1.27 ± .10	0.40 ± .02[d]
74-1 FFC025	XRF (Dugolinsky, 1975)[b]	4	6.9 ± .8	26.6 ± 1.0	2.5 ± .3	---	1.13 ± .04	1.78 ± .12	0.51 ± .11
	A.A. (Frank, this work)	4	6.0 ± .3	30.7 ± .6	2.9[c]	0.21 ± .01	1.24 ± .03	1.58 ± .03	0.48 ± .02[d]
74-02 BC 2	XRF (Dugolinsky, 1975)[b]	1	6.7	28.1	2.3	---	1.12	1.67	0.53
	A.A. (Frank, this work)	3	5.6 ± .3	31.7 ± 1.6	1.5[c]	0.23 ± .01	1.27 ± .06	1.49 ± .08	0.33 ± 0[d]

[a] Meylan, M.A., MS Thesis, Florida State University, 1968.

[b] Dugolinsky, B.K., University of Hawaii, personal communication.

[c] Single analysis.

[d] Duplicate analysis by XRF.

[e] Standards for calibration of Ti analysis by XRF in this work (additional standards used for Ti not included here).

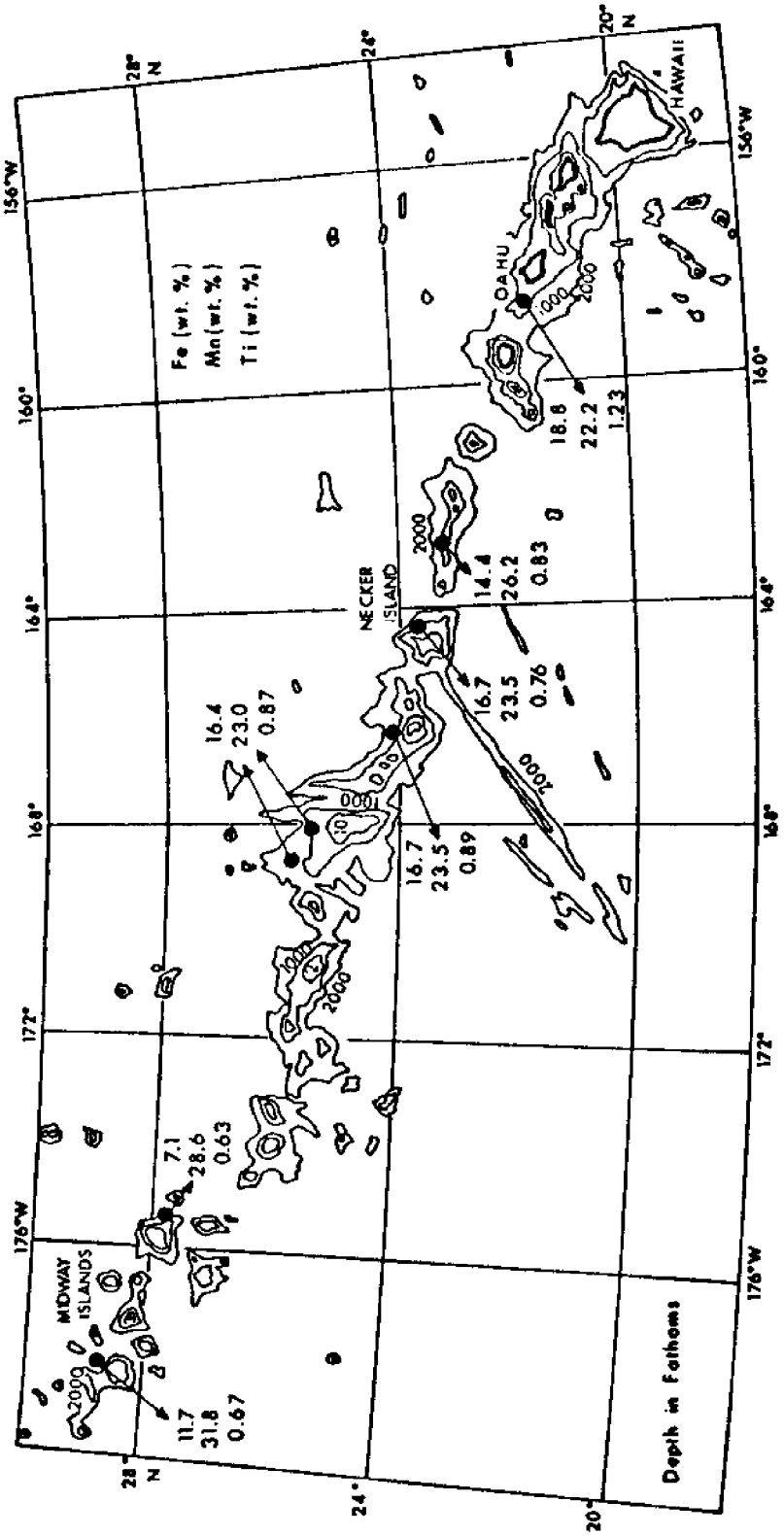

Figure 13. Mean iron, manganese, and titanium contents in Fe-Mn deposits from individual dredge hauls in the Hawaiian Archipelago.

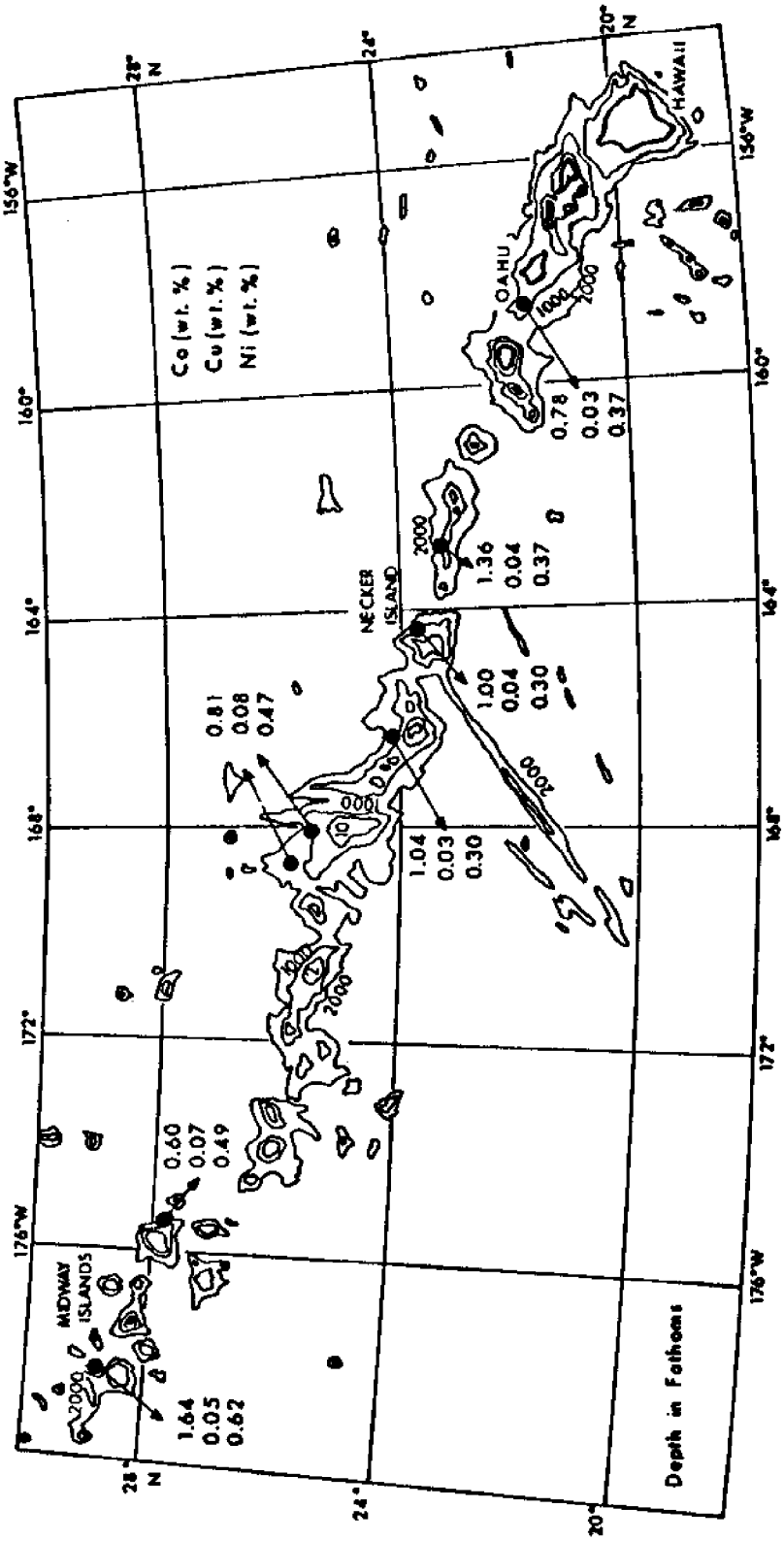

Figure 14. Mean cobalt, copper, and nickel contents in Fe-Mn deposits from individual dredge hauls in the Hawaiian Archipelago.

correlation of Co with Al in particular tends to emphasize the problems of selecting a pure Fe-Mn oxide sample excluding the substrate material. Presumably the Al represents contamination by alumino-silicate clay minerals.

Data for the Fe-Mn crusts from the northwestern part of the Archipelago were averaged and compared with data from the Kauai Channel. The results of this comparison are presented in Table 4. From these data, it is evident that there is an apparent increase in Co, Cu, Ni, and Mn and a decrease in Fe and Ti in crusts and nodules from the leeward islands compared to those from the Kauai Channel. This trend follows that of greater Fe-Mn crustal thicknesses ($\sim$ 2.5 cm) generally observed in the leeward chain compared to those in the Kauai Channel ($\sim$ 5 mm). In addition, this table gives the weighted average of these two regions (i.e., average for the Hawaiian Archipelago) of all ferromanganese crusts analyzed in this study.

The degree of enrichment of elements in the manganese crusts relative to the associated substrates is variable between stations but the enrichment sequence is generally in the order Co (89) > Mn (79) > Ni (13)> Cu (2.8) > Fe (0.8) > Ti (0.3) > Al(0.04), the enrichment factor for the sample showing the highest enrichment (sample KK-72 Midway DG20) being shown in parentheses. Significantly, Co shows the greatest degree of enrichment. High Co contents have been commonly observed in manganese crusts from seamount environments such as the intermontane belt between Tahiti and the Cook Islands (up to 2.23%) (Glasby and Lawrence, 1974) and the Mid-Pacific Mountains (average 1.127%) (Cronan, 1972), although Co contents from plateau environments such as the Campbell Plateau (0.19- >1.0%) (Glasby and Summerhayes, 1975), Blake Plateau (0.3%) (Manheim, 1972), Manihiki Plateau (0.51%) (Horn et al., 1973), and Aghulas Bank (0.19-0.45%) (Summerhayes and Willis, 1975) are not so high. These elevated Co concentrations may reflect the substitution of Co^{3+} for Mn^{4+} in the δ-MnO_2 phase epitaxially intergrown with $FeOOH \cdot nH_2O$ in the manganese crusts in these well-oxygenated types of environment (Burns, 1976). This mode of entry is supported by the observed Mn-Co correlation in the manganese crusts. The much greater degree of enrichment of Mn relative to Fe in the crusts relative to the substrate reflects the strong separation of these elements from each other (Krauskopf, 1957) and indicates the Mn is derived from some source other than leaching of the substrate (probably direct deposition from seawater). The degree of enrichment of Fe in the crust relative to the substrate varies between 0.8 and 2.2 and suggests that the iron may be derived at least partially from weathering or alteration of the substrate. Ti and Al are both present in lower concentrations in the crusts than in the substrate, suggesting that these elements are both derived principally from the volcanic substrate, Al being subject to a greater degree of weathering (of the original alumino-silicate minerals) or dilution by other elements in the manganese crusts than is Ti. Finally, a surprising feature of the data is the extremely low Cu contents of the crusts and the slight enrichment of this element in crusts relative to substrate. Glasby (in press), for example, has

TABLE 4

CHEMICAL ANALYSIS OF HAWAIIAN MANGANESE CRUSTS AND NODULES

Element	Crusts and Nodules: Kauai Channel-Waho Shelf	Crusts and Nodules: Northwestern Archipelago	Crusts and Nodules: Entire Archipelago	Typical Substrate (KK-72 Midway DG 32E)	Average Sediment*
Fe (%)	18.8	14.9	17.3	10.4	17.19
Mn (%)	22.2	24.9	23.2	0.4	---
Co (ppm)	7841	9733	8569	96	1406
Cu (ppm)	323	621	438	251	501
Ni (ppm)	3745	4450	4016	250	1388
Ti (%)	1.23	0.81	1.07	1.65	---

*From manganese crustal zone off Kauai (on a carbonate-free basis) (Burnett, 1971).

shown that the Ni/Cu ratios of South Pacific nodules are typically of the order of 2, whereas these deposits frequently have values exceeding 10. Part of the reason for this may be the complete absence of diagenetic contribution of this element from the underlying sediment or the low biological productivity of the region. However, the reasons for these low Cu contents in the manganese crusts relative to the substrate are not understood.

According to Burnett (1971), the Fe, Cu, Ni, and Co contents of bottom sediments from the area off Kauai where manganese crusts are found is substantially higher than from other areas around Hawaii where manganese crusts do not occur (171900, 501, 1388, 406 versus 118600, 190, 197, 115 p.p.m. on a carbonate-free basis, respectively). This may indicate that the factors which lead to an enrichment of these elements in the manganese crusts also lead to an enrichment of these elements in the associated sediments. Significantly, however, the manganese crusts do not show the marked fractionation of Mn from Fe and associated trace elements similar to that observed in some shallow basin environments such as Loch Fyne, Scotland, and Jervis Inlet, British Columbia (Ku and Glasby, 1972), indicating that diagenetic processes (i.e., remobilization of manganese in the sediment column) such as observed in the basinal-type environments do not occur here. This conclusion is not unexpected since in most cases the manganese crust is dredged directly off rock outcrop and there is no underlying sedimentary column.

From the results listed in Table 4 and Appendix 3, it is evident that iron oxides are more abundant than manganese oxides in the substrate. Moreover, the iron oxides were always observed stratigraphically below manganese oxides in the crusts. These two factors conform with the hypothesis of Goldberg and Arrhenius (1958) that iron-catalyzed manganese precipitation is an important step in nodule genesis in this type of environment. It appears that the distribution and supply of ferruginous oxides is more varied than that of manganese as indicated by the depositional schemes of iron oxides in worm tubes (Morgenstein, 1974). In each case, ferruginous precipitation occurs prior to manganese accretion and the rate of iron oxide supply is assumed to control the rate of manganese accretion. The iron oxides are supplied to the sediment-water interface by both chemical and physical processes. Among those mechanisms recognized in the Kauai Channel sediments (and presumably other sediments of the Hawaiian Archipelago) for the entrapment of iron oxides in the substrate are:

1) Biochelation of iron oxides by allelids and other fauna.

2) Authigenic mineralization of volcanoclastic material such as sideromelane, palagonite, olivine, and magnetite.

3) Primary precipitation on and formation of selective ferruginous coatings on small detritus at the sediment-water interface.

4) Reworking of ferruginous bearing sediments such as iron oxide-coated smectites and their subsequent physical deposition in

microsediment traps, such as the surfaces of mineral grains and carbonate clastics.

Figure 15 shows the Mn/Fe ratios for the area sampled. There appear to be three distinct regions of these ratios. The first is in the Kauai Channel, having a value of 1.18. The second is in the leeward islands from 162°W to 170°W, with values between 1.40 and 1.82. The third is in the area of the Midway Islands, 174°W to 179°W, with values of 2.72 and 4.03. According to Meylan and Goodell (1976), high Mn/Fe ratios enhance the formation of the manganese mineral todorokite which tends to concentrate Cu and Ni in deep-sea nodules. Todorokite, however, appears as an identifiable mineral in only two of the samples studied, MW1-12 #14A and KK-72 Midway DG 24, which have ratios of 4.03 and 1.50, respectively. These samples do not, however, appear to be enriched in Cu and Ni compared to other samples in the same area. In addition, sample Mn 75-02 #17, which has a reasonably high Mn/Fe ratio (1.67) and high Cu and Ni contents, shows no detectable todorokite. A possible explanation for these facts is that the Fe content, which is about twice that reported in todorokite-rich deep-sea nodules, ties up too much Mn as δ-MnO_2/$FeOOH \cdot nH_2O$ epitaxial intergrowths to permit identifiable amounts of todorokite form.

SUMMARY AND CONCLUSIONS

Geologic and Geochemical Aspects

Ferromanganese oxide accumulations have been found in all parts of the Hawaiian Archipelago. These accumulations occur predominantly as crusts overlying lithified sandstones, siltstones, and mudstones. There are occasional manganese nodules with centers of generally large altered rock fragments, and some iron-encrusted carbonate sands and silts. Based on presently available information, the most extensive and economically promising deposit is found in the leeward island chain, KK-72 Midway DG 32 and 33 (25°33'N, 168°40'W at depths between 1000-1570 m). This deposit also includes large discrete nodules in contrast to the predominance of crustal accumulations found at other sites. The thicknesses of the crusts were found to vary considerably over short distances and on all types of substrate throughout the archipelago with no distinct pattern. However, it was found that the crustal accumulations in the leeward chain were on the average thicker (10-25 mm) than those of the Kauai Channel area (2-5 mm).

Although the relative importance of the various factors controlling manganese crustal distribution and thickness in the Hawaiian Archipelago cannot be assessed on the basis of presently available information, the following would clearly be important:

1) Age of the seamount or island on which it formed.

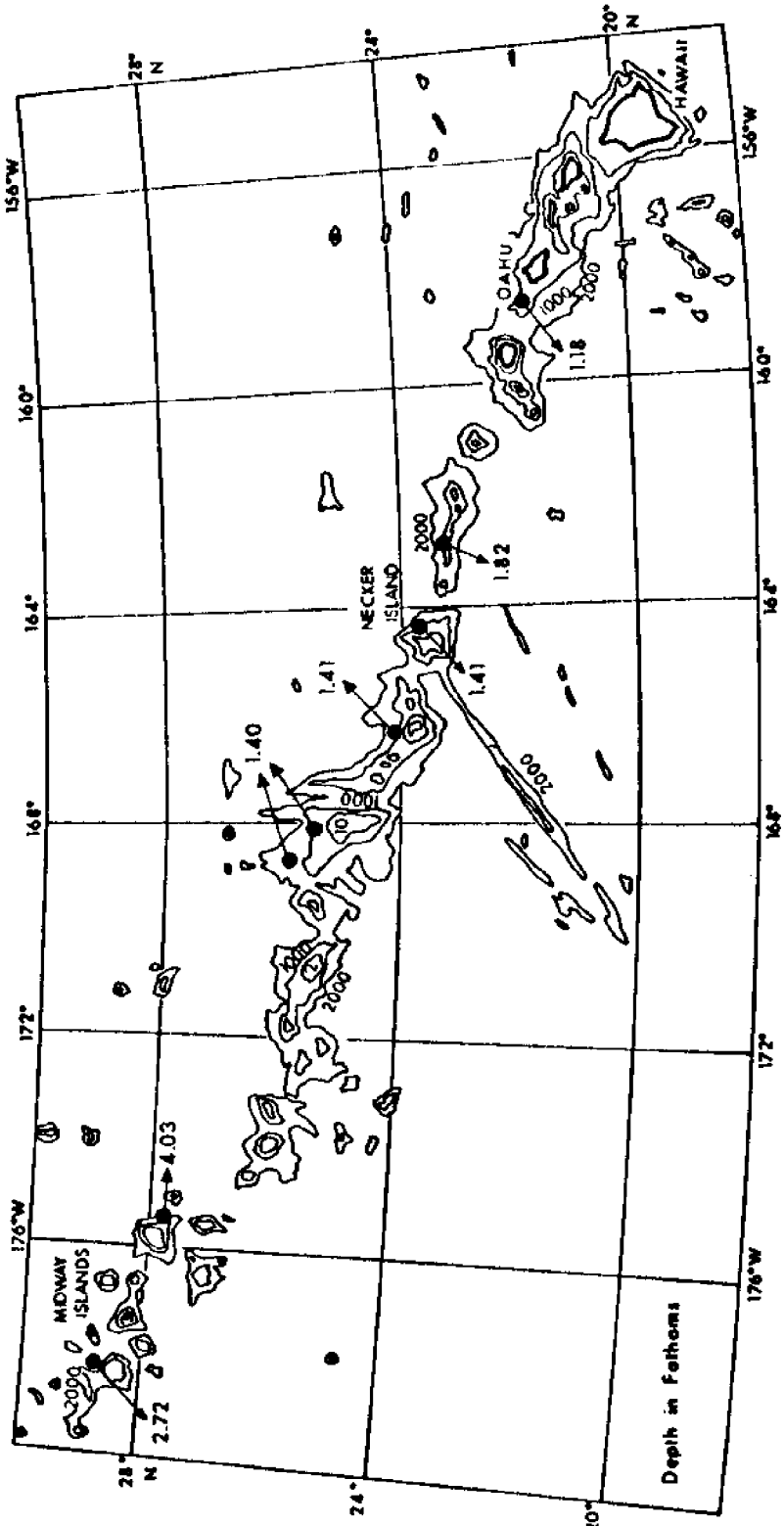

Figure 15. Mean manganese/iron ratios in Fe-Mn deposits from individual dredge hauls in the Hawaiian Archipelago.

2) The extent of isostatic subsidence and sea level changes.

3) Lithology and degree of weathering of the substrate. This includes the relative importance of basalt and coral as the substrate for manganese accumulation.

4) The extent of subaerial and submarine erosion.

5) Submarine canyon formation.

6) Submarine terrace formation.

7) Rate of pelagic sedimentation.

The dominant iron and manganese phases in the ferromanganese crust accumulations were found to be X-ray amorphous oxides and hydroxides. The most abundant crystalline manganese phase was δ-MnO_2, while todorokite was only rarely identifiable. No crystalline authigenic iron phase occurred in recognizable quantities. The substrates on which the oxide crusts precipitate were typically basaltic volcanics in various stages of alteration, and consisted of variable proportions of plagioclase feldspar, pyroxene, phillipsite, montmorillonite, and other less abundant minerals.

The ferromanganese crusts in the Hawaiian Archipelago were found to have greater concentrations of Mn, Fe, Co, Cu and Ni relative to the volcanogenic substrate, attesting to the probability that these elements are concentrated in the oxide portion of the sediment during halmyrolysis reactions. Titanium, on the other hand, was always found to be less concentrated in the oxide crust relative to its associated substrate. Although sample coverage was incomplete, a slight trend toward increasing Co, Cu, Ni, and Mn and decreasing Fe and Ti concentrations was found to the northwest along the leeward island chain. This seems to follow that of increasing Fe-Mn crustal thickness in the same direction. Of the elements of potential economic interest only Co was found in high enough concentration (0.86% average for the Archipelago) to be economically interesting. Nickel and manganese, at 0.40% and 23.2%, respectively, are of potential secondary interest.

Although no distinct interelement relationships were found, three regions with distinct Mn/Fe ratios were observed. These were low Mn/Fe (1.18) in the Kauai Channel, intermediate Mn/Fe (1.40-1.82) around 177°W, and high Mn/Fe (2.72 and 4.03) around the Midway Islands. Although todorokite tends to be enhanced by high Mn/Fe ratios, this mineral was only rarely observed. Presumably the higher Fe content of these Hawaiian ferromanganese crusts (approximately twice that of todorokite-rich deep-sea nodules) ties up too much Mn as δ-MnO_2/$FeOOH \cdot nH_2O$ intergrowths to permit significant amounts of this mineral to form.

In summary, it is proposed that the general factors promoting ferromanganese crust accumulation in the Hawaiian Archipelago are: (1) an oxidizing environment with adequate water circulation so that sufficient

concentrations of divalent manganese in the water column can pass over ferruginous sites of accretion; (2) the presence of strong bottom-currents, steep slopes, or slow rates of pelagic sedimentation so that the accreting manganese does not become covered by sediment; and (3) the formation of terraces that can act as traps for basaltic and other rubble on which the manganese crusts can accrete.

Furthermore, it is proposed that the source for manganese is more varied than just divalent manganese in seawater. Additional sources for manganese probably also include a small supply from hydrating basaltic debris such as sideromelane and palagonite, and an upward migration of manganese in the sedimentary column. Although the latter two mechanisms do not seem to be of extreme importance in the Hawaiian Archipelago sediments, it appears from other workers (Bonatti and Nayudu, 1965; Lynn and Bonatti, 1965; Boström and Peterson, 1966, among others) that they are significant in the deep-sea sediments. According to Moore (1966), the lack of manganese encrustations on samples of young lava from the active submarine rift zone east of the Kilauea volcano indicates that manganese is not formed by rapid accumulation from submarine volcanic exhalations, but may be released in part during palagonitization.

Economic Considerations

The economic potential of ferromanganese crusts in the Hawaiian Archipelago is of immediate concern in the justification of further investigations of this deposit as well as being a primary goal of this study. However, an answer to the basic question of what will be economic versus what is potentially economic is not yet apparent. A recent article by Cook (1976), for example, describes some of the considerations necessary in the evaluation of geologic resources. Considerations are centered around the concept of profit, that is, the "ultimate limit to exploitation" occurs when it takes more energy to find, recover, and process a resource than the net "energy profit" produced. In essence, the world will not "run out" of geologic resources before they become too expensive to exploit. Advances in technology to save the energy input have steadily lowered the ore grades produced and increased the availability of required resources.

Ferromanganese deposits in both deep-sea and shallow-water settings are faced with technological gaps in recovery aspects at present, as well as uncertainties as to the legal regime that would permit exploitation in international waters. Vague production dates of a few years to a few tens of years are projected by most observers. However, the resource potential for deep-sea nodule deposits is being actively evaluated by mining companies from a number of industralized nations. The possible importance of this untapped resource in a global context of dwindling high grade reserves, unstable third-world countries, and environmental protection is without question. A comparison between deep-sea nodule deposits from the northern equatorial Pacific and crusts from

TABLE 5

FERROMANGANESE DEPOSIT PARAMETERS RELEVANT TO EXPLOITATION

	N.E. EQUATORIAL	HAWAIIAN ARCHIPELAGO	CONTINENTAL ORE CUT-OFF GRADE (COOK, 1976)
CHEMISTRY†			
Ti	0.4	1.1	10.0
Cu	1.3	0.04	0.35
Ni	1.5	0.40	0.90
Co	0.2	0.86	0.20
Mn	30.0	23.2	25.0
Fe	6.0	17.3	20.0
GEOGRAPHY			
water depth	4000-5000 m	750-2000 m	
distance from market	3700 km	3700 km	
legal ownership	unclear	USA*	
distance from port	1800-3700 km	180 km	
DEPOSIT CHARACTERISTICS			
form	nodules	crusts	
distribution	variable	variable	
substrate	soft	hard	
boundaries	gradational	gradational	
bathymetry	smooth to rough	moderately rough	

*Subject to acceptance of the Archipelagic doctrine at the U.N. Law of the Sea Conference.

†Elemental concentrations in percent.

the Hawaiian Archipelago is therefore presented in Table 5 along with the cut-off grade for continental reserves mined in 1975.

The principal metal of economic interest in Hawaiian waters is cobalt (∿ 0.86% by weight), which is present in concentrations four times higher on average than in deep-sea deposits and the cut-off grade for recoverable continental reserves. According to Archer (1976), without the production of cobalt from manganese nodules, there could be a gap between world supply and demand for this metal by 1985. Nickel and manganese are of potential secondary interest, assuming the current world value of these metals will have increased by the time these deposits are exploited. Although copper and nickel are of principal interest in deep-sea nodules, cobalt recovered in the processing of these nodules may result in increased supply and affect its exploitation in other areas, such as the "shallow" environment of the Hawaiian Archipelago.

Several common problems face marine mining in both deep and shallow water environments, the most important of which is the ability to extract the ferromanganese ore from its position on the sea floor economically. To date, mining systems have not been fully developed to carry out this operation, particularly in archipelagic terrains, the greatest effort having been devoted to deep-sea deposits. Standard dredging techniques are definitely too slow and retain too much substrate material. The nature of deposits in the Hawaiian Archipelago is quite different from deep-sea deposits, and therefore would require special techniques to mine this resource effectively. Further investigations are critical to the development of a suitable mining system for this shallow, rugged environment. Assessment of bottom coverage of ferromanganese oxides throughout the archipelago, together with studies of the associated substrate and the bathymetric setting (micro-relief) at potential mining areas must be completed before a reasonable estimate of mining system costs versus potential ore profitability can be made. It is probable that only the most favorable ferromanganese deposits in the Hawaiian Archipelago could ever be considered of economic interest and these would have to satisfy the criteria of being nodular (as opposed to crusts), having relatively thick coatings of manganese oxides (up to 25 mm in the leeward chain) and high Co contents, and being in a region of relatively smooth topography. Principal attention in the future should therefore be directed to establishing the location and extent of these deposits, if they occur.

REFERENCES

Andrews, J. E. (1972), Distribution of manganese nodules in the Hawaiian Archipelago. p. 61 in Manganese Nodule Deposits in the Pacific, Department of Planning and Economic Development, State of Hawaii, 220 pp.

Andrews, J. E., C. W. Landmesser, and M. Morgenstein (1973), Hawaii Institute of Geophysics data banks for manganese collections and hydration-rind dating. Hawaii Inst. Geophys. Rept. HIG-73-5, 187 pp.

Archer, A. A. (1976), Prospects for the exploitation of manganese nodules: The main technical, economic and legal problems. CCOP/SOPAC Tech. Bull., 2, 21.

Belshé, J. C. (1968), Oceanic sediments sampled during 1964-1967 in the Hawaiian Archipelago. Hawaii Inst. Geophys. Rept. HIG-68-7, 52 pp.

Bonatti, E., and Y. R. Nayudu (1965), The origin of manganese nodules on the ocean floor. Am. J. Sci., 263, 17.

Boström, K., and M. N. A. Peterson (1966), Precipitates from hydrothermal exhalations on the East Pacific Rise. Econ. Geol., 61, 1258.

Bouma, A. H. (1963), Sedimentology of Some Flysch Deposits. Elsevier, Amsterdam, 168 pp.

Burnett, W. C. (1971), Trace element variations in some Central Pacific and Hawaiian sediments. Hawaii Inst. Geophys. Rept. HIG-71-6, 112 pp.

Burns, R. G. (1976), The uptake of cobalt into ferromanganese nodules, soils and synthetic manganese (IV) oxides. Geochim. Cosmochim. Acta, 40, 95.

Burns, V. M., and R. G. Burns (1973), Manganese nodule authigenesis: Mechanism for nucleation and growth. Abstr. Progr. Ann. Mtg. Geol. Soc. Am., 5, 564 (Abst.).

Clague, D. A., G. B. Dalrymple, and R. Moberly (1975), Petrography and K-Ar ages of dredged volcanic rocks from the western Hawaiian Ridge and the southern Emperor Seamount chain. Bull. Geol. Soc. Am., 86, 991.

Cook, E. (1976), Limits to exploitation of nonrenewable resources. Sci., N.Y., 191, 677.

Cronan, D. S. (1972), Regional geochemistry of ferromanganese nodules in the world ocean. P. 19 in D. R. Horn, Editor, Ferromanganese Deposits on the Ocean Floor, National Science Foundation, Washington, D.C., 293 pp.

Cronan, D. S. (in press), Deep-sea deposits: Distribution and geochemistry. In G. P. Glasby, Editor, Marine Manganese Deposits, Elsevier, Amsterdam.

Dalrymple, G. B., M. A. Lanphere, and E. D. Jackson (1974), Contributions to the petrography and geochronology of volcanic rocks from the leeward Hawaiian islands. Bull. Geol. Soc. Am., 85, 727.

Dalrymple, G. B., E. A. Silver, and E. D. Jackson (1973), Origin of the Hawaiian islands. Am. Scient., 61, 294.

Dugolinsky, B. K. (1976), Chemistry and morphology of deep-sea manganese nodules and the significance of associated encrusted protozoans on nodule growth. Unpubl. Ph.D. dissertation, University of Hawaii, 228 pp.

Dymond, J., P. E. Biscaye, and R. W. Rex (1974). Eolian origin of mica in Hawaiian soils. Bull. Geol. Soc. Am., 85, 37.

Fein, C. D., and M. Morgenstein (1972), Microprobe analysis of manganese crusts from the Hawaiian Archipelago. P. 41 in J. E. Andrews et al., Investigations of Ferromanganese Deposits from the Central Pacific, Hawaii Inst. Geophys. Rept. HIG-72-23, 133 pp.

Fein, C. D., and M. Morgenstein (1973), Microprobe analysis of manganese crusts from the Hawaiian Archipelago. EOS Trans. Am. Geophys. Un., 54(4), 340 (Abstr.).

Fein, C. D., and M. Morgenstein (1974), New artificial reefs on Oahu. P. 51 in Proc. Int. Conf. Artificial Reefs, TAMU-SG-74-103, Center for Marine Resources, Texas A&M Univ., College Station, Texas.

Furumoto, A. S., N. J. Thompson, G. P. Woollard (1965), The structure of Koolau volcano from seismic refraction studies. Pacific Sci., 19, 306.

Glasby, G. P. (in press), Manganese nodules in the South Pacific: A review. N. Z. J. Geol. Geophys.

Glasby, G. P., and P. Lawrence (1974), Manganese deposits in the South Pacific Ocean: Cobalt content. N.Z. Oceanogr. Inst. Chart. Misc. Ser. 38.

Glasby, G. P., and C. P. Summerhayes (1975), Sequential deposition of authigenic marine minerals around New Zealand: Paleoenvironmental significance. N.Z. J. Geol. Geophys., 18, 477.

Goldberg, E. D., and G. O. S. Arrhenius (1958), Chemistry of Pacific pelagic sediments. Geochim. Cosmochim. Acta, 13, 153.

Hamilton, E. L. (1957), Marine geology of the southern Hawaiian Ridge. Bull. Geol. Soc. Am., 68, 1011.

Horn, D. R., B. M. Horn, and M. N. Delach (1973), Ocean manganese nodules metal values and mining sites. Tech. Rept. Int. Decade Ocean Explor., 4, 57 pp.

Inman, D. L., W. R. Gayman, and D. C. Cox (1963), Littoral sedimentary processes on Kauai, a subtropical high island. Pacific Sci., 17, 106.

Jackson, E. D. (1976), Linear volcanic chains on the Pacific plate. P.319 in G. H. Sutton, M. H. Manghnani, and R. Moberly, Editors, The Geophysics of the Pacific Ocean Basin and Its Margin, Monogr. 19, Am. Geophys. Un.

Jackson, E. D., and T. L. Wright (1970), Xenoliths in the Honolulu volcanic series, Hawaii. J. Petrol., 11, 405.

Jackson, E. D., E. A. Silver, and G. B. Dalrymple (1972), Hawaiian-Emperor chain and its relation to Cenozoic circumpacific tectonics. Bull. Geol. Soc. Am., 83, 601.

Jeffrey, P. G. (1970), Chemical Methods of Rock Analysis. Pergamon, Oxford, 507 pp.

Krauskopf, K. B. (1957), Separation of manganese from iron in sedimentary processes. Geochim. Cosmochim. Acta, 12, 61.

Kroenke, L. W. (1965), Seismic reflection studies of sediment thickness around the Hawaiian Ridge. Pacific Sci., 19, 157.

Ku, T.-L., and G. P. Glasby (1972), Radiometric evidence for the rapid growth rate of shallow-water, continental margin manganese nodules. Geochim. Cosmochim. Acta, 36, 699.

Landmesser, C. W., and M. E. Morgenstein (1973), Survey and mapping of manganese deposits in the Hawaiian Archipelago. P. 93 in M. Morgenstein, Editor, Papers on the Origin and Distribution of Manganese Nodules in the Pacific and Prospects for Exploration, State of Hawaii, Dept. Planning and Econ. Devel., Honolulu, 175 pp.

Lynn, D. C., and E. Bonatti (1965), Mobility of manganese in diagenesis of deep-sea sediments. Mar. Geol., 3, 457.

Macdonald, G. A., and T. Katsura (1964), Chemical composition of Hawaiian lavas. J. Petrol., 5, 82.

Manheim, F. T. (1965), Manganese-iron accumulations in the shallow marine environment. P. 217 in Symposium on Marine Chemistry, Occ. Publs. Univ. Rhode Island, 3.

Manheim, F. T. (1972), Composition and origin of manganese iron nodules and pavements on the Blake Plateau (abstr.). P . 105 in D. R. Horn, Editor, Ferromanganese Deposits on the Ocean Floor, National Science Foundation, Washington, D.C., 293 pp.

Mathewson, C. C. (1969), Bathymetry of the north insular shelf of Molokai island, Hawaii, from surveys by the USC and GSS McArthur. Hawaii Inst. Geophys. Rept. HIG-69-21, 9 pp.

Menard, H. W., and T. Atwater (1968), Changes in direction of seafloor spreading. Nature, 219, 463.

Meylan, M. A. (1968), The mineralogy and geochemistry of manganese nodules from the Southern Ocean. Unpubl. M.S. thesis, Florida State University, 177 pp.

Meylan, M. A., and H. G. Goodell (1976), Chemical composition of manganese nodules from the Pacific-Antarctic Ocean, Drake Passage and Scotia Sea: Relation to ferromanganese oxide mineralogy and nucleus type. CCOP/SOPAC Tech. Bull., 2, 99.

Moberly, R., and R. L. Larson (1975), Mesozoic magnetic anomalies, oceanic plateaus, and seamount chains in the Northwestern Pacific Ocean. p. 945 in Initial Reports of the Deep Sea Drilling Project, vol. 32, U.S. Govt. Printing Office, Washington, D.C., 980 pp.

Moore, J. G. (1965), Petrology of deep-sea basalt near Hawaii. Am. J. Sci., 263, 40.

Moore, J. G. (1966), Rate of palagonitization of submarine basalt adjacent to Hawaii. Prof. Paper U.S. Geol. Surv., 550D, 163.

Moore, J. G., and R. S. Fiske (1969), Volcanic substructure inferred from dredge samples and ocean-bottom photographs, Hawaii. Bull. Geol. Soc. Am., 80, 1191.

Morgenstein, M. (1972a), Manganese accretion at the sediment-water interface at 400 to 2400 meters depth, Hawaiian Archipelago. P. 131 in D. R. Horn, Editor, Ferromanganese Deposits on the Ocean Floor, National Science Foundation, Washington, D.C., 293 pp.

Morgenstein, M. (1972b), Sedimentary diagenesis and rates of manganese accretion on the Waho Shelf, Kauai Channel, Hawaii. P. 1 in J. E. Andrews et al., Investigations of Ferromanganese Deposits from the Central Pacific, Hawaii Inst. Geophys. Rept. HIG-72-23.

Morgenstein, M. (1973). Sedimentary diagenesis and rates of manganese accretion on the Waho Shelf, Kauai Channel, Hawaii. EOS Trans. Am. Geophys. Un., 54(4), 339 (Abstr.).

Morgenstein, M. (1974), Sedimentary diagenesis and manganese accretion on submarine platforms, Kauai Channel, Hawaii. Unpubl. Ph.D. dissertation, University of Hawaii, 172 pp.

Morgenstein, M., and J. E. Andrews (1971), Manganese resources in the Hawaiian region. Mar. Technol. Soc. J., 5(6), 27.

Stearns, H. T. (1966), Geology of the State of Hawaii. Pacific Books, Palo Alto, Calif., 266 pp.

Stearns, H. T. (1974), Submerged shorelines and shelves in the Hawaiian Islands and a revision of some of the eustatic emerged shorelines. Bull. Geol. Soc. Am., 85, 795.

Strange, W. E., G. P. Woollard and J. C. Rose (1965), An analysis of the gravity field over the Hawaiian Islands in terms of crustal structure. Pacific Sci., 19, 381.

Summerhayes, C. P., and J. P. Willis (1975), Geochemistry of manganese deposits in relation to environment on the sea floor around southern Africa. Mar. Geol., 18, 159.

Walker, J. L. (1964), Pedogenesis of some highly ferruginous formations in Hawaii. Hawaii Inst. Geophys. Rept. HIG-64-10, 406 pp.

APPENDIX 1: SAMPLE DESCRIPTION

Sample	Water Depth (Meters)	Lat. N.	Long. W.	Proportion Manganese (Mn) vs. Substrate (S)	Description
MOANA WAVE CRUISE NO. 74-01					
MW1-3 #1A	1170	21°34.4'	158°22.8'	Mn > S	Nodule, about 2.5 cm diameter with less than 1 mm thick Mn crust.
MW1-3 #1B	1170	21°34.4'	158°22.8'	S	Altered volcanic substrate, white to dark gray color.
MW1-4 #2	795	21°43.6'	158°17.5'	Mn	Nodules, 6-10 cm diameter with Mn crust 1-2 mm thick.
MW1-5 #3A	920	21°40.5'	158°27.4'	Mn	Nodules, 2.5 cm diameter with 2-3 mm Mn crust.
MW1-5 #3B	920	21°40.5'	158°27.4'	S	Basalt substrate along with partly altered volcanics, brown-gray with bright yellow-brown patches.
MW1-5 #4A	920	21°40.5'	158°27.4'	Mn	Oblong nodules (5-15 cm long diam.) with 1 mm Mn crust having pebbly surface.
MW1-5 #4B	920	21°40.5'	158°27.4'	S	Basalt substrate along with partly altered volcanics, brown-gray with yellow-brown spots.
MW1-6 #5A	985	21°41.5'	158°29.7'	Mn	Nodule, 2.5 cm diameter with 4 mm Mn crust.
MW1-6 #5B	985	21°41.5'	158°29.7'	S	Altered volcanic nucleus, reddish brown color.

Sample	Water Depth (Meters)	Lat. N.	Long. W.	Proportion Manganese (Mn) vs. Substrate (S)	Description
MW1-6 #6	985	21°41.5'	158°29.7'	Mn	Nodule, 2.5 cm diameter with 3 mm Mn crust.
MW1-7 #7A	800	21°44.4'	158°37.1'	Mn	Pebble-sized nodules; four 0.5 cm diam. and rounded; one oblong (2.5 x 1.5 cm).
MW1-7 #7B	800	21°44.4'	158°37.1'	S	Altered volcanic nucleus, reddish brown color.
MW1-8 #8A	1340	21°51.0'	158°41.2'	Mn	Piece of 10 x 15 x 5 cm nodule, broken at one end. Mn crust 1-2 mm thick with pebbly surface.
MW1-8 #8B	1340	21°51.0'	158°41.2'	S	Altered volcanic substrate, bright yellow-brown and tan color.
MW1-9 #9A	1840	21°54.3'	158°38.1'	Mn	Broken nodule with 3-4 mm Mn crust having rough pebbly surface.
MW1-9 #9B	1840	21°54.3'	158°38.1'	S	Basalt nucleus with outer portion partly altered (brown to yellow-brown patches).
MW1-10 #10A	1985	21°57.9'	158°36.6'	Mn	Nodule, 20 cm diameter with 5 mm Mn crust having pebbly surface.
MW1-10 #10B	1985	21°57.9'	158°36.6'	S	Basalt nucleus.
MW1-10 #11A	1985	21°57.9'	158°36.6'	Mn	Nodule, 2.5 cm diameter with 4-5 mm Mn crust.

Sample	Water Depth (Meters)	Lat. N.	Long. W.	Proportion Manganese (Mn) vs. Substrate (S)	Description
MW1-10 #11B	1985	21°57.9'	158°36.6'	S	Basalt nucleus.
MW1-10 #12A	1985	21°57.9'	158°36.6'	Mn	Nodules, 5 cm diameter with 2 mm Mn crust having pebbly surface.
MW1-10 #12B	1985	21°57.9'	158°36.6'	S	Altered volcanic nucleus with colors mottled; yellow, bright yellow-buff, tan and black.
MW1-12 #13A	1120	21°46.9'	158°44.6'	Mn > S	Flattened nodules, 2.5-5.0 cm long with 1 mm Mn crust having pebbly surface.
MW1-12 #13B	1120	21°46.9'	158°44.6'	S	Altered volcanic nucleus, yellow-brown color.
MW1-12 #14A	1120	21°46.9'	158°44.6'	Mn	Nodule, 2.5 cm diameter with 3 mm Mn crust.
MW1-12 #14B	1120	21°46.9'	158°44.6'	S	Altered volcanic nucleus, yellow-gray color.
MW1-13 #15	1175	21°47.2'	158°36.9'	Mn < S	Very thin, patchy crust and staining over altered volcanic substrate and inside vesicules. Substrate medium brown in color.
KANA KEOKI CRUISE NO. 75-11-10					
Mn 75-02 #1	1265	21°50'	158°40'	Mn < S	Pebbly Mn crust, 0.5 mm thick. Substrate, rock fragments in beige tuff matrix.

Sample	Water Depth (Meters)	Lat. N.	Long. W.	Proportion Manganese (Mn) vs. Substrate (S)	Description
Mn 75-02 #2A	1265	21°50'	158°40'	Mn >> S	Smooth to botryoidal Mn crust, 2 mm thick.
Mn 75-02 #2B	1265	21°50'	158°40'	Mn << S	Friable yellow-brown coarse sandy tuff.
Mn 75-02 #4A	1265	21°50'	158°40'	Mn > S	Botryoidal Mn crust, 4-5 mm thick.
Mn 75-02 #4B	1265	21°50'	158°40'	Mn << S	Friable brown granular lithic tuff.
Mn 75-02 #5A	1265	21°50'	158°40'	Mn >> S	Botryoidal Mn crust, 4-6 mm thick.
Mn 75-02 #5B	1265	21°50'	158°40'	Mn << S	Friable yellow-brown; coarse sandy tuff, with bore holes.
Mn 75-02 #6	1265	21°50'	158°40'	Mn > S	Botryoidal Mn crust; 5-6 mm top (?) and 2-3 mm bottom(?). Substrate friable gray-brown lithic tuff.
Mn 75-02 #7	1265	21°50'	158°40'	Mn > S	Smooth to low relief botryoidal Mn crust, 0-3 mm thick. Substrate friable gray-brown coarse sandy tuff.
Mn 75-02 #8A	1265	21°50'	158°40'	Mn > S	Smooth to botryoidal Mn crust, 3-10 mm thick.
Mn 75-02 #8B	1265	21°50'	158°40'	Mn << S	Friable gray-brown to red-brown coarse sandy tuff.
Mn 75-02 #10	1910	21°55.4'	158°47.7'	Mn < S	Botryoidal Mn crust, 1-2 mm thick. Substrate friable mottled altered coarse sandy tuff.

Sample	Water Depth (Meters)	Lat. N.	Long. W.	Proportion Manganese (Mn) vs. Substrate (S)	Description
Mn 75-02 #11	1910	21°55.4'	158°47.7'	Mn < S	Microbotryoidal Mn crust, about 1 mm thick. Substrate, mottled altered coarse sandy tuff.
Mn 75-02 #12	1910	21°55.4'	158°47.7'	Mn << S	Manganese staining on upper surface. Substrate, gray-white kaolinized(?) sandy tuff.
Mn 75-02 #13	1115	21°52.3'	158°49.4'	Mn < S	Smooth to low relief botryoidal, about 2 mm thick (top?). Substrate, gray-brown to red-brown partially altered granular tuff.
Mn 75-02 #14	1115	21°52.3'	158°49.4'	Mn = S	Botryoidal Mn crust (smaller & higher relief on side with thinnest Mn), 1-3 mm thick. Substrate partially friable yellow-brown to gray-brown coarse sandy tuff.
Mn 75-02 #15A	1115	21°52.3'	158°49.4'	Mn > S	Botryoidal Mn crust, 3 mm thick.
Mn 75-02 #15B	1115	21°52.3'	158°49.4'	Mn << S	Friable yellow-brown coarse sandy tuff.
Mn 75-02 #16	1115	21°52.3'	158°49.4'	Mn < S	Smooth to low relief microbotryoidal Mn crust, 0.5-1 mm thick. Substrate, partially friable gray-brown coarse sandy tuff. Tube (5 mm diam.) in substrate has partial clay infilling.
Mn 75-02 #17	1115	21°52.3'	158°49.4'	Mn >> S	Smooth Mn crust, about 1 mm thick. Substrate gray vesicular porphyritic basalt.

Sample	Water Depth (Meters)	Lat. N.	Long. W.	Proportion Manganese (Mn) vs. Substrate (S)	Description
Mn 75-02 #18	1644	20°54.0'	157°21.4'	Mn << S	Incomplete Mn stain on substrate of pumice which is partially altered and infilled with brown clay.
Mn 75-02 #21A	1220	20°8.2'	156°15.9'	Mn < S	Microbotryoidal and low relief botryoidal Mn crust, about 1 mm thick.
Mn 75-02 #21B	1220	20°8.2'	156°15.9'	Mn << S	Friable partially altered mottled coarse sandy tuff (obviously crystal tuff containing mineral crystals just below Mn crust).
Mn 75-02 #22	1220	20°8.2'	156°15.9'	Mn < S	Smooth Mn crust, about 1 mm thick. Substrate interbedded fine-grained yellow brown tuff and Mn crusts (latter up to 2 mm thick).
Mn 75-02 #24	1220	20°8.2'	156°15.9'	Mn << S	Mn and Fe staining on substrate of olive-brown tuff.
Mn 75-02 #25	1220	20°8.2'	156°15.9'	Mn << S	Mn crust 0.5 mm thick on substrate of friable yellow-brown coarse sandy tuff with 1.5 cm diam., 7 cm long Mn-encrusted tube.
Mn 75-02 #26	1220	20°8.2'	156°15.9'	S	No apparent Mn. Substrate cream-colored pisolitic (kaolinized?) granular tuff(?); knobby upper surface has reddish-gray and orange staining.

Sample	Water Depth (Meters)	Lat. N.	Long. W.	Proportion Manganese (Mn) vs. Substrate (S)	Description
KANA KEOKI CRUISE NO. 72-07-02					
KK-72 Midway DG 20A	875-1090	28°49.0'	178°57.0'	Mn >> S	Mn crust up to 1 cm thick. Surface smooth or with large suppressed botryoids.
KK-72 Midway DG 20B	875-1090	28°49.0'	178°57.0'	Mn << S	Red-brown and yellow-brown cavernous volcanic fragment (lava surface?).
KK-72 Midway DG 24	1050-1125	27°42.1'	175°41.0'	Mn > S	Mn crust 2 mm thick with botryoidal surface intergrown with outermost rock layer. Substrate highly altered tuffaceous volcanic conglomerate boulder.
KK-72 Midway DG 32A	1450-1570	25°40.5'	168°41.8'	Mn >> S	Top crust? — Flat Mn nodule probably originally about 10 x 9 x 2 cm. Upper crust thicker (~ 1 cm), having prominent botryoids. Lower crust thinner (~ 0.5 cm), having large suppressed botryoids. Substrate yellow-brown tuffaceous siltstone < 0.5 cm thick.
KK-72 Midway DG 32B	1450-1570	25°40.5'	168°41.8'	Mn >> S	Bottom crust?
KK-72 Midway DG 32C	1450-1570	25°40.5'	168°41.8'	Mn + S (Bulk sample)	Bulk sample: Flattened, ellipsoidal Mn nodule, 8.5 x 5.5 x 4.5 cm. Crust 1-1.5 cm thick with botryoidal surface. Substrate buff-colored tuffaceous siltstone.

Sample	Water Depth (Meters)	Lat. N.	Long. W.	Proportion Manganese (Mn) vs. Substrate (S)	Description
KK-72 Midway DG 32D	1450-1570	25°40.5'	168°41.8'	Mn >> S	Fragment of Mn nodule, probably originally tabular and about 15 cm max. diam. Crust up to 1 cm thick with botryoidal surface. Substrate, sample DG 32E.
KK-72 Midway DG 32E	1450-1570	25°40.5'	168°41.8'	Mn << S	Buff-colored tuffaceous siltstone with subconchoidal fracture. Mn and Fe staining on fracture surfaces. Mn crust, sample DG 32D.
KK-72 Midway DG 33A	1000-1150	25°29.3'	168°39.4'	Mn >> S	Fragments of Mn nodule, probably originally 5.5 cm max. diam. having ellipsoidal shape. Crust up to 13 mm thick with smooth well-developed botryoids; zone of yellow-brown laminae just below crust surface. Substrate similar to sample DG 33C.
KK-72 Midway DG 33B	1000-1150	25°29.3'	168°39.4'	Mn >> S	Flattened ellipsoidal nodule, 6.5 x 5 x 4.5 cm. Crust 1.3-1.5 cm thick with yellow-brown laminae and botryoidal surface. Substrate, sample DG 33C.
KK-72 Midway DG 33C	1000-1150	25°29.3'	168°39.4'	Mn << S	Tuffaceous siltstone(?), partially replaced by Mn; size 2.5 x 2 x 1 cm. Mn crust, sample DG 33B.
KK-72 Midway DG 43	1060-1170	24°17.5'	166°43.8'	Mn > S	Mn crust 1-2 mm thick with large Mn-encrusted burrows. Substrate burrowed buff-colored tuffaceous siltstone.

Sample	Water Depth (Meters)	Lat. N.	Long. W.	Proportion Manganese (Mn) vs. Substrate (S)	Description
KK-72 Midway DG 47A	775-960	23°49.0'	164°25.2'	Mn >> S	Mn crust 1-7 mm thick; surface prominently botryoidal. Mn partly penetrates and indurates upper 1-2 mm of substrate.
KK-72 Midway DG 47B	775-960	23°49.0'	164°25.2'	Mn << S	Altered yellow-brown to red-brown friable tuffaceous sandstone.
KK-72 Midway DG 49	850-892	23°22.0'	163°34.0'	Mn >> S	Mn crust up to 6 mm thick. Surface smooth to suppressed botryoidal, with micro-granular texture in crevasses. Substrate large volcanic conglomerate fragment.

APPENDIX 2

MINERALOGY OF MANGANESE CRUSTS AND SUBSTRATES (OR NUCLEI) SELECTED FOR X-RAY DIFFRACTION ANALYSIS

	--MINERAL PRESENCE--		
Sample	Definite	Probable	Possible
MW1-3 #1A Crust + Nucleus	Plagioclase Montmorillonite	Pyroxene	δ-MnO_2
MW1-3 #1B Nucleus	Plagioclase Calcite Montmorillonite Pyroxene		Ilmenite
MW1-4 #2 Crust		δ-MnO_2	
MW1-5 #3A Crust		δ-MnO_2	
MW1-5 #3B Nucleus	Plagioclase	Pyroxene	Hematite
MW1-5 #4A Crusts		δ-MnO_2	Todorokite
MW1-5 #4B Nuclei	Plagioclase	Pyroxene	Phillipsite
MW1-6 #5A Crust		δ-MnO_2	
MW1-6 #5B Nucleus	Plagioclase		Calcite
MW1-6 #6 Crust		δ-MnO_2	
MW1-7 #7A Crusts		δ-MnO_2	
MW1-7 #7B Nuclei	Plagioclase		Pyroxene
MW1-8 #8A Crust		δ-MnO_2 Plagioclase	

	--MINERAL PRESENCE--		
Sample	Definite	Probable	Possible
MW1-8 #8B Nucleus	Phillipsite Plagioclase	Pyroxene Montmorillonite	Quartz
MW1-9 #9A Crust		δ-MnO_2	Quartz Plagioclase
MW1-9 #9B Nucleus	Plagioclase	Pyroxene	Phillipsite
MW1-10 #10A Crust		δ-MnO_2 Quartz	
MW1-10 #10B Nucleus	Plagioclase Pyroxene	Phillipsite	Quartz
MW1-10 #11A Crust		δ-MnO_2	Quartz
MW1-10 #11B Nucleus	Plagioclase Pyroxene Calcite	Phillipsite	Olivine
MW1-10 #12A Crust		δ-MnO_2	
MW1-10 #12B Nucleus	Plagioclase	Pyroxene Calcite	Olivine
MW1-12 #13A Crusts + nuclei	Plagioclase	Phillipsite Illite	δ-MnO_2 Calcite Pyroxene Quartz
MW1-12 #13B Nucleus	Plagioclase	Illite Pyroxene Phillipsite	Quartz
MW1-12 #14A Crust	Todorokite	δ-MnO_2	
MW1-12 #14B Nucleus	Plagioclase Pyroxene	Calcite Olivine	
MW1-13 #15 Substrate + crust	Plagioclase	Phillipsite Calcite Pyroxene	Montmorillonite

	--MINERAL PRESENCE--		
Sample	Definite	Probable	Possible
Mn75-02 #1 Substrate + crust	Plagioclase	Pyroxene	Quartz
Mn75-02 #2A Crust		δ-MnO_2	
Mn75-02 #2B Substrate	Plagioclase Phillipsite	Pyroxene	Quartz
Mn75-02 #4A Crust + substrate	Plagioclase		δ-MnO_2
Mn75-02 #4B Substrate	Plagioclase Pyroxene	Phillipsite	Calcite Quartz
Mn75-02 #5A Crust		δ-MnO_2	
Mn75-02 #5B Substrate	Plagioclase Phillipsite Pyroxene		Calcite Quartz Montmorillonite
Mn75-02 #6 Crust + substrate		Plagioclase	δ-MnO_2
Mn75-02 #7 Crust + substrate	Plagioclase		δ-MnO_2
Mn75-02 #8A Crust + substrate			δ-MnO_2 Plagioclase
Mn75-02 #8B Substrate	Plagioclase Pyroxene	Phillipsite	Montmorillonite Calcite
Mn75-02 #10 Substrate + crust		Illite Plagioclase	δ-MnO_2 Phillipsite Calcite
Mn75-02 #11 Substrate + crust		Illite	Quartz Calcite δ-MnO_2
Mn75-02 #12 Substrate	Calcite		Quartz

	--MINERAL PRESENCE--		
Sample	Definite	Probable	Possible
Mn75-02 #13 Substrate + crust	Plagioclase	Quartz	Phillipsite
Mn75-02 #14 Crust + substrate	Plagioclase		Phillipsite Pyroxene δ-MnO_2
Mn75-02 #15A Crust + substrate	Plagioclase	δ-MnO_2	Calcite
Mn75-02 #15B Substrate	Montmorillonite Plagioclase	Pyroxene	Quartz
Mn75-02 #16 Substrate + crust	Plagioclase Phillipsite Pyroxene	Calcite	Illite
Mn75-02 #17 Crust		δ-MnO_2	
Mn75-02 #18 Substrate	Plagioclase Pyroxene	Phillipsite	Calcite
Mn75-02 #21A Substrate + crust	Olivine	Montmorillonite	δ-MnO_2 Plagioclase
Mn75-02 #21B Substrate	Olivine		Montmorillonite
Mn75-02 #22 Substrate + crust	Montmorillonite	δ-MnO_2	
Mn75-02 #24 Substrate		Montmorillonite	δ-MnO_2
Mn75-02 #25 Substrate	Olivine Montmorillonite		Illite
Mn75-02 #26 Substrate	Calcite Aragonite		
KK-72 Midway DG 20A Crust		δ-MnO_2	

	--MINERAL PRESENCE--		
Sample	Definite	Probable	Possible
KK-72 Midway DG 20B Substrate	Plagioclase	Kaolinite Pyroxene	Montmorillonite
KK-72 Midway DG 24 Crust + substrate	Todorokite Phillipsite	δ-MnO_2	Quartz
KK-72 Midway DG 32A Crust	Quartz	δ-MnO_2	
KK-72 Midway DG 32B Crust		δ-MnO_2	Todorokite Quartz
KK-72 Midway DG 32C Crust + nucleus	Glass	δ-MnO_2	Quartz Phillipsite
KK-72 Midway DG 32D Crust		δ-MnO_2 Quartz	
KK-72 Midway DG 32E Nucleus	Montmorillonite		δ-MnO_2
KK-72 Midway DG 33A Crust		δ-MnO_2	Quartz
KK-72 Midway DG 33B Crust		δ-MnO_2	Todorokite Plagioclase
KK-72 Midway DG 33C Nucleus	Montmorillonite	Illite Maghemite	
KK-72 Midway DG 43 Crust + substrate		δ-MnO_2	Quartz

	--MINERAL PRESENCE--		
Sample	Definite	Probable	Possible
KK-72 Midway DG 47A Crust		δ-MnO_2	
KK-72 Midway DG 47B Substrate	Goethite	Maghemite and/or Magnetite	Phillipsite
KK-72 Midway DG 49 Crust		δ-MnO_2	

APPENDIX 3

CHEMISTRY OF MANGANESE CRUSTS AND SUBSTRATES (OR NUCLEI) SELECTED FOR ANALYSIS

Sample		Fe (%)	Mn (%)	Al (%)	Co (ppm)	Cu (ppm)	Ni (ppm)	Ti (%)
MW1-4 #2	Crust	20.3	24.3	---	11002	260	3368	1.21
MW1-5 #3A	Crust	22.4	24.3	---	9232	151	2624	1.13
MW1-6 #5A	Crust	sample lost						1.58
MW1-6 #6	Crust	19.5	27.4	---	11658	253	4428	1.12
MW1-8 #8A	Crust	17.5	22.4	---	8674	283	4014	1.17
MW1-9 #9A	Crust	21.8	19.5	---	5910	260	2810	1.27
MW1-10 #10A	Crust	19.3	24.0	---	7964	266	3714	---
MW1-10 #11A	Crust	20.8	22.1	---	7397	383	3623	1.33
MW1-12 #14A	Crust	17.2	25.8	---	7611	692	6924	---
Mn75-02 #1	Substrate + crust	11.6	4.7	5.4	1775	248	1437	1.49
Mn75-02 #2A	Crust	19.3	24.6	---	7982	240	3412	1.04
Mn75-02 #2B	Substrate	8.6	3.0	---	123	122	331	1.27
Mn75-02 #4A	Crust + substrate	18.3	21.6	---	7824	357	3173	1.25
Mn75-02 #5A	Crust	20.5	21.6	---	6679	274	2642	1.20
Mn75-02 #5B	Substrate	9.4	3.2	---	106	129	322	1.21
Mn75-02 #6	Crust + substrate	17.1	18.0	---	5541	319	2824	1.31
Mn75-02 #7	Crust + substrate	15.8	13.0	---	3877	379	2820	1.36

Sample		Fe (%)	Mn (%)	Al (%)	Co (ppm)	Cu (ppm)	Ni (ppm)	Ti (%)
Mn75-02 #8A	Crust + substrate	18.6	22.5	---	7644	256	3404	1.08
Mn75-02 #8B	Substrate	10.0	2.7	---	88	120	351	1.31
Mn75-02 #11	Substrate + crust	22.6	7.6	---	616	530	3753	0.25
Mn75-02 #12	Substrate	2.7	1.2	---	26	27	113	0.11
Mn75-02 #14	Crust + substrate	13.6	8.9	---	3779	251	1488	1.35
Mn75-02 #15A	Crust + substrate	16.0	17.2	---	5381	196	3036	1.04
Mn75-02 #17	Crust	16.3	27.2	---	8561	588	7105	1.00
Mn75-02 #21A	Substrate + crust	10.8	14.9	3.4	550	115	1189	1.23
Mn75-02 #21B	Substrate	---	---	---	---	---	---	1.25
Mn75-02 #22	Substrate + crust	10.8	8.2	---	210	123	336	1.51
KK-72 Midway DG20A	Crust	11.7	31.8	0.3	16441	531	6245	0.67
KK-72 Midway DG20B	Substrate	13.9	0.4	7.6	185	188	468	2.35
KK-72 Midway DG24	Crust + substrate	7.1	28.6	1.8	5970	664	4884	0.63
KK-72 Midway DG32A	Crust	16.9	23.5	0.8	8000	700	4114	0.93
KK-72 Midway DG32B	Crust	15.9	21.6	1.4	7413	1246	5920	0.97
KK-72 Midway DG32C	Crust + nucleus (bulk sample)	15.7	19.8	1.7	6662	842	4425	1.12
KK-72 Midway DG32D	Crust	17.5	22.0	1.0	7711	684	3488	0.89
KK-72 Midway DG32E	Nucleus	10.4	0.4	6.8	96	251	250	1.65
KK-72 Midway DG33A	Crust	15.4	23.7	1.2	7753	686	5252	0.73

Sample		Fe (%)	Mn (%)	Al (%)	Co (ppm)	Cu (ppm)	Ni (ppm)	Ti (%)
KK-72 Midway DG33B	Crust	16.2	24.4	1.2	10025	683	4921	0.83
KK-72 Midway DG33C	Nucelus	10.0	8.0	5.8	1990	594	3025	1.64
KK-72 Midway DG43	Crust + substrate	16.7	23.5	0.8	10408	291	2986	0.89
KK-72 Midway DG47A	Crust	16.7	23.5	0.9	10027	350	2987	0.76
KK-72 Midway DG47B	Substrate	18.0	3.4	4.7	380	322	1567	1.15
KK-72 Midway DG49	Crust	14.4	26.2	0.5	13584	371	3699	0.83